A major purpose of the Technical Information Center is to provide the broadest dissemination possible of information contained in DOE's Research and Development Reports to business, industry, the academic community, and federal, state and local governments.

Although a small portion of this report is not reproducible, it is being made available to expedite the availability of information on the research discussed herein.

CONF-8307102--1

LA-UR--83-2851

DE84 001017

Los Alamos National Laboratory is operated by the University of California for the United States Department of Energy under contract W-7405-ENG-36.

TITLE RECENT DEVELOPMENTS IN THE UNDERSTANDING OF PION-NUCLEUS SCATTERING

AUTHOR(S) Mikkel B. Johnson

SUBMITTED TO The 1983 International Symposium on Nucleon-Nucleon Interaction and Nuclear Many-Body Problems, Beijing, China, July-August, 1983.

Los Alamos National Laboratory
Los Alamos, New Mexico 87545

RECENT DEVELOPMENTS IN THE UNDERSTANDING OF PION-NUCLEUS SCATTERING

Mikkel B. Johnson

Los Alamos National Laboratory
Los Alamos, New Mexico 87545

ABSTRACT

A development of the theory of pion-nucleus scattering is given in a field theoretical framework. The theory is designed to describe pion elastic scattering and single- and double-charge exchange to isobaric analog states. An analysis of recent data at low and resonance energies is made. Strong modifications to the simple picture of the scattering as a succession of free pion-nucleon interactions are required in order to understand the data. The extent to which the experiment is understood in terms of microscopic theory is indicated.

The basic problem in the theory of hadron-nucleus scattering as viewed in nuclear physics is to arrive at a formulation which addresses the fundamental issues, which permits quantitative answers to certain practical questions, and which is readily solvable. The last requirement makes the task very difficult. In the specific case of pion physics at medium energies, nuclear physics is challenged to go beyond the traditional framework and to solve the many-body problem of a quantum field interacting with a collection of nucleon sources. The final result must describe the interplay among the nuclear, pion, and Δ_{33} dynamics. The coupling among these sectors of the problem can become fairly intricate, but the theory must seriously address all three if it is to be able to separate the fundamental issues from uncertainties in nuclear structure, which one would like to probe as a practical application. For example, the pion has a special sensitivity to neutron densities, and one hopes that this sensitivity can be exploited to study separately and in detail the neutron component of ground and excited nuclear states.

In these lectures I will discuss a theory of elastic scattering and single- and double-charge exchange to isobaric analog states which addresses these issues. The lectures will emphasize the pedagogical development and will utilize time-dependent perturbation methods to find a suitable theory of the optical potential based on a field theoretical description. In order to bring together elastic, single- and double-charge exchange, isospin invariance will be incorporated at a basic level of the theory. Interpretation of recent LAMPF data in this theoretical framework will be made.

I. Basic Theory

Traditional multiple scattering theories[1] are not well justified for describing pion-nucleus scattering. These theories assume that the dynamics can be adequately described by potentials and that the number of projectile particles is conserved. This is clearly not the case in pion-nucleus scattering, because pion number may increase or decrease by one unit at any time: during intermediate time intervals any number of pions may be present. Thus, one would like to build up the final result in terms of the absorption and emission amplitudes of a meson from a nucleon (and its first excited state, Δ_{33}), with one objective being to learn new details of how this coupling occurs.

In order to be able to describe scattering of a projectile under these circumstances one must use more powerful techniques. The appropriate tool from many-body theory is the Green's function[2] $G_{\alpha'\alpha}(t' - t)$, which gives the amplitude to remove a pion in state α' from the ground state of the system at time t' when it is inserted at time t in state α. The formal definition of this Green's function is

$$G_{\alpha'\alpha}(t' - t) \equiv i^{-1}\langle 0|\, T[a_{\alpha'}(t')a^{+}_{\alpha}(t)]\,|0\rangle \tag{1}$$

where $|0\rangle$ is the interacting ground state, $a^{+}_{\alpha}(t)$ is the pion creation operator in the Heisenberg representation and T is the time-ordering operator. The advantage of the Green's function is that it lends itself to diagrammatic analysis, which means that the "bookkeeping" for its numerical evaluation is especially simple. The Green's function applies to the case of multiple scattering in both potential theory and field theory.

I would like to give now an intuitive derivation of the equation of motion for the pion wave function $\psi(x,t)$. The derivation is based on the existence of the Green's function but does not require a specific dynamical model. I wish to make the following assumptions:

(a) we know the pion wave function for large negative times $t = t_0 + -\infty$;

$$\psi_0(\underset{\sim}{x}) = \psi(x,t_0) = e^{i(\underset{\sim}{k}\cdot\underset{\sim}{x}_0 - Et_0)} \quad . \tag{2}$$

(b) we know the amplitude $S(x',x)$ for propagation of the pion from $x = (\underset{\sim}{x},t)$ to x' without exciting the medium;

(c) we know the amplitude $F(x',x)$ for the propagation of the excited medium.

The amplitude $\psi(x')$ is related to $\psi_0(x)$ by the principle of superposition, i.e., $\psi(x')$ is obtained from $\psi_0(x)$ by summing over all interfering histories for the evolution of the system,

$$\psi(x') = \int d^3x_0 \sum_i A_i(\underset{\sim}{x}'t'; \underset{\sim}{x}_0 t_0)\psi_0(\underset{\sim}{x}_0 t_0) \quad , \tag{3}$$

where the A_i describe a history in which the pion interacts with the system i times through F (see Fig. 1). Because we know the amplitudes for propagation of the pion without exciting the medium and for propagation of the excited medium, we have

$$A_0 = S(x',x) \quad , \tag{4}$$

$$A_1 = \int\int d^4x_1' d^4x_1 \; S(x',x_1') \; F(x_1',x_1) \; S(x_1,x_0) \quad , \text{ and} \tag{5}$$

$$A_2 = \int\ldots\int d^4x_1' \; . d^4x_2 \; S(x',x_1') \; F(x_1',x_1) \; S(x_1,x_2') \; F(x_2',x_2) \; S(x_2,x_0) \quad . \tag{6}$$

If we call the sum of all these amplitudes $G_{x_1'x_0}(t' - t_0)$,

$$G_{\underset{\sim}{x}',\underset{\sim}{x}_0}(t' - t_0) = \sum_i A_i(x',x_0) \quad , \tag{7}$$

which is appropriate by definition of the Green's function, then it is possible to evaluate G by solving the integral equation,

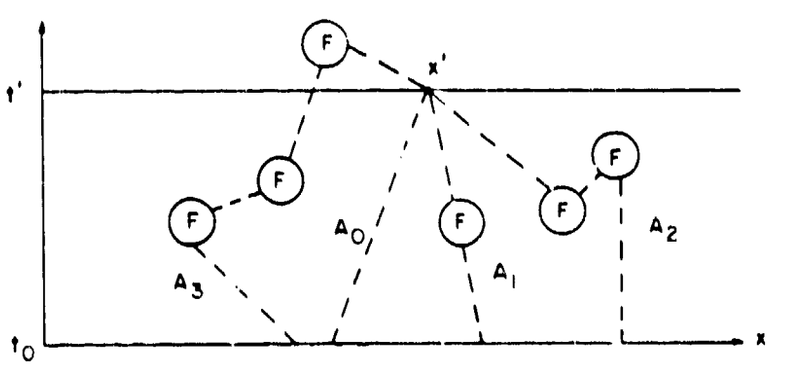

Fig. 1. Illustrating alternative histories A_i by which the pion (dashed line) may propagate from t_0 to t. Alternative amplitudes are summed coherently to get the complete amplitude for finding the meson at $(\underset{\sim}{x}',t')$.

$$G_{x',x_0}(t' - t_0) = S(x',x_0) + \iint d^4x_1' d^4x_1 S(x',x_1')F(x_1',x_1)G_{x_1',x_0}(t_1 - t_0) \quad . \quad (8)$$

That Eq. (8) is equivalent to the sum of A_1 is most easily seen by repeatedly inserting the left-hand side of Eq. (8) into the right-hand side.

Now, to find the equation of motion for $\psi(x,t)$ we make use of the fact that the wave equation for a free pion is the Klein-Gordon equation, so that

$$(\frac{\partial}{\partial t^2} - \nabla^2 + \mu^2)S(x',x) \equiv (\Box + \mu^2)S(x',x) = -i\delta(\underset{\sim}{x}' - \underset{\sim}{x})\delta(t' - t) \quad . \quad (9)$$

Applying $\Box + \mu^2$ to Eq. (8) and using Eqs. (3), (7), and (9) we find

$$[\Box + \mu^2 - i \int d^4x_1 \, F(x',x_1)] \, \psi(x_1,t_1) = 0 \text{ for } t' > t_0 = -\infty \quad . \quad (10)$$

Equation (10) is the desired result. By taking the Fourier transform we find that the wave function $\psi_\omega(x)$ for a pion of energy ω satisfies the familiar Klein-Gordon scattering equation

$$[-\nabla^2 + \mu^2 + \int d^3x' \langle \underset{\sim}{x}|U(\omega)|\underset{\sim}{x}'\rangle] \, \psi_\omega(\underset{\sim}{x}') = \omega^2 \psi_\omega(x) \quad , \quad (11)$$

where the optical potential U is just the Fourier transform of the amplitude of the pion-excited medium,

$$\langle \underset{\sim}{x}'|U(\omega)|\underset{\sim}{x}\rangle \equiv -i\int_{-\infty}^{\infty} d(t' - t)e^{i\omega(t'-t)}F(\underset{\sim}{x}'t'; \underset{\sim}{x}t) \quad . \quad (12)$$

We have used the result that F can depend only on the time difference $t' - t$ due to invariance under time translation. The elastic-scattering amplitude is obtained from ψ in the usual way. Understanding the meaning of $\psi(x,t)$ in terms of the pictures in Fig. 1 is useful for determining how to use $\psi(x,t)$ in the calculation of other observables such as inelastic scattering.

One easily sees by referring to Fig. 1 that the theory which we have constructed does not preserve the number of pions across a given time interval. Thus, physics embodied in Eq. (11) goes beyond that of traditional multiple-scattering potential theories. Examples of formulations which begin with potentials and use one of the traditional multiple-scattering theories are given in Ref. 3. The

equation of motion in these theories is often the relativistic Schroedinger equation. The isobar-hole model of Ref. 4 makes use of a generalization of Schroedinger dynamics to treat the coupling between the pion and isobar-hole excitations. Not only is the physical basis of the relativistic Schroedinger equation different from that of the Klein-Gordon equation, but in practice they can lead to different results.[5]

The main problem is now to find a theory of the amplitude $F(x',x)$ for the propagation of the excited medium. We must introduce a dynamical model for this purpose. In this lecture I want to pick a simple model for the meson-nucleon coupling and for the nuclear dynamics, but I want to insist that the model address the new aspect, that pions are emitted and absorbed as single quanta. In particular, I want to treat the nucleons of the nucleus as fixed sources of the meson field. The static theory is believed to approximately describe a theory including nucleon recoil under suitable conditions,[6] and therefore, the static theory can be useful for making estimates. The extent to which these conditions are satisfied is an important issue in practice, so that the static assumption will have to be relaxed later to make quantitative comparisons to experimental data. The main point is that the extension to include nucleon recoil is not one of a conceptual nature and that the structure of the theory is almost unchanged. The extension does add much aggravation to the practical implementation, however.

With these caveats clearly in mind, I will now describe a Hamiltonian H which has many of the desired properties. We shall take H to have the three pieces,

$$H = H_{OB} + H_{OM} + H' \quad . \tag{13}$$

The baryon sector is described by

$$H_{OB} = \sum_{ij} b_i^+ b_j (m_i \delta_{ij} + u_{ij}) \quad , \tag{14}$$

where b_i^+ is a creation operator for a nucleon or a Δ_{33} of mass m_i at position $\underset{\sim}{r}_i$. We envision the Δ_{33} as an independent degree of freedom as it would be in the quark model. We have included a counter term u_{ij} which may be used for purposes of renormalization. The meson sector is described similarly by

$$H_{OM} = \sum_{k} a_k^+ a_k \omega_k \quad , \tag{15}$$

where $\omega_k \equiv (k^2 + m_k^2)^{1/2}$ and a_k^+ creates a meson of quantum numbers "k", which will stand for momentum, isospin,.... In these lectures,

we will allow the meson to be a pion or a ρ meson. The coupling among these degrees of freedom is specified by

$$H' = \sum_{ijn} [a_n b_j^\dagger b_i \, V^{ji}(k) + \text{H.C.}] \quad , \tag{16}$$

where the interactions $V^{ji}(k)$ may be described diagrammatically as in Fig. 2. Specific expressions for π and ρ couplings to nucleons are

$$V_\pi^{NN} = (f_{\pi NN}/m_\pi) \underset{\sim}{\sigma} \cdot \underset{\sim}{k} \, \underset{\sim}{\tau} \cdot \underset{\sim}{\alpha} \, v_{\pi NN}(k) \quad \text{and} \tag{17}$$

$$V_\rho^{NN} = (f_{\rho NN}/m_\rho) \, \underset{\sim}{\varepsilon} \cdot \underset{\sim}{\sigma} \times \underset{\sim}{k} \, \underset{\sim}{\tau} \cdot \underset{\sim}{\alpha} \, v_{\rho NN}(k) \quad , \tag{18}$$

where $\underset{\sim}{\sigma}$ and $\underset{\sim}{\tau}$ are Pauli matrices in spin and isospin space, $\underset{\sim}{\alpha}$ is a vector representing the isospin quantum number of the meson, $\underset{\sim}{\varepsilon}$ is the polarization vector of the meson and the $v(k)$ are form factors. The standard value for $f_{\pi NN}^2/4\pi$ is 0.08, and the ρ-meson coupling will be taken as the "strong" value,[7]

$$f_{\rho NN}^2/f_{\pi NN}^2 \cdot m_\pi^2/m_\rho^2 = 2 \quad . \tag{19}$$

Similarly, the π and ρ coupling to the isobar Δ_{33} are

$$V_\pi^{\Delta\Delta} = (f_{\pi\Delta\Delta}/m_\pi) \, \underset{\sim}{\Sigma} \cdot \underset{\sim}{k} \, \Theta \cdot \underset{\sim}{\alpha} \, v_{\pi\Delta\Delta}(k) \quad \text{and} \tag{20}$$

$$V_\rho^{\Delta\Delta} = (f_{\rho\Delta\Delta}/m_\rho) \, \underset{\sim}{\varepsilon} \cdot \underset{\sim}{\Sigma} \times \underset{\sim}{k} \, \underset{\sim}{\Theta} \cdot \underset{\sim}{\alpha} \, v_{\rho\Delta\Delta}(k) \quad , \tag{21}$$

where $\underset{\sim}{\Sigma}$ and $\underset{\sim}{\Theta}$ are the Δ_{33} spin and isospin operators,

$$\Sigma^2 |\Delta_{33}\rangle = \frac{15}{4} |\Delta_{33}\rangle \quad ,$$

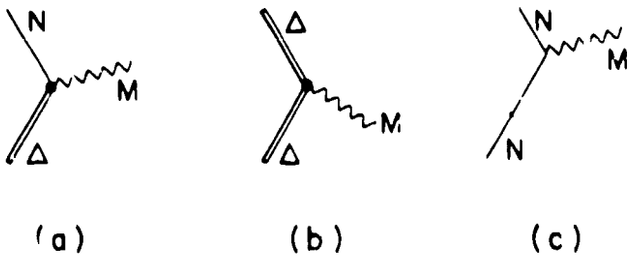

(a) (b) (c)

Fig. 2. Examples of meson-baryon co plings employed in these lectures.

and similarly for isospin. The value for the coupling of the pion to the Δ_{33} can be related to $f_{\pi NN}$ by SU(2) × SU(2) quark model arguments[8] which give

$$(f_{\pi\Delta\Delta}/f_{\pi NN})^2 = \frac{16}{25} \quad . \tag{22}$$

Similarly, the coupling of the ρ meson to the Δ leads to the relationship

$$f_{\rho\Delta\Delta}/f_{\rho NN} = f_{\pi\Delta\Delta}/f_{\pi NN} \quad . \tag{23}$$

Finally, transitions between nucleons and Δ_{33} may be described by

$$V_\pi^{N\Delta} = (f_{\pi N\Delta}/m_\pi)\ \underset{\sim}{S} \cdot \underset{\sim}{k}\ \underset{\sim}{T} \cdot \underset{\sim}{\alpha}\ v_{\pi N\Delta}(k) \quad \text{and} \tag{24}$$

$$V_\rho^{N\Delta} = (f_{\rho N\Delta}/m_\rho)\ \underset{\sim}{\varepsilon} \cdot \underset{\sim}{S} \times \underset{\sim}{k}\ \underset{\sim}{T} \cdot \underset{\sim}{\alpha}\ v_{\rho N\Delta}(k) \quad , \tag{25}$$

where SU(2) × SU(2) symmetry again relate the pion coupling to that of nucleons

$$f^2_{\pi N\Delta}/f^2_{\pi NN} = 72/25 \quad \text{and} \tag{26}$$

$$f_{\rho N\Delta}/f_{\pi NN} = f_{\pi N\Delta}/f_{\pi NN} \quad . \tag{27}$$

In Eqs. (24) and (25) $\underset{\sim}{S}$ and $\underset{\sim}{T}$ are transition spin and isospin operators, respectively, defined by[9]

$$\left\langle \tfrac{3}{2}\ M \middle| \underset{\sim}{S} \cdot \underset{\sim}{k} \middle| \tfrac{1}{2}\ m \right\rangle = \sum_{m_k} C\left(\tfrac{3}{2}\ M;\ \tfrac{1}{2}\ m;\ 1m_k\right) \hat{e}^*(m_k) \cdot \underset{\sim}{k} \quad , \tag{28}$$

where the unit vector $\hat{e}^*(m_k)$ is defined through the relation

$$\hat{k} \cdot \hat{e}^*(m_k) = \sqrt{4\pi/3}\ Y_{1m_k}(\hat{k}) \quad . \tag{29}$$

A similar definition holds for the transition isospin operator. The vectors α in Eqs. (17) through (25) have the same representation as $\hat{e}(m_k)$ of Eq. (29), i.e., a π^+ is represented by $\hat{e}(m = +1) \equiv \hat{\alpha}_{\pi^+}$. The $\underset{\sim}{S}$ and $\underset{\sim}{T}$ operators are related to projection operators, e.g.,

$$\underset{\sim}{T}^+ \cdot \hat{\alpha}\ T \cdot \hat{\beta} = \delta_{\alpha\beta} - \frac{1}{3}\ \underset{\sim}{\tau} \cdot \hat{\alpha}\ \underset{\sim}{\tau} \cdot \hat{\beta} \tag{30}$$

projects onto total isospin 3/2 of the pion-nucleon system, and similarly

$$\frac{3}{4\pi}\,\underset{\sim}{S}^{+}\cdot k'\,\underset{\sim}{S}\cdot\underset{\sim}{k}=\frac{3}{4\pi kk'}\left(\underset{\sim}{k}\cdot\underset{\sim}{k}'-\frac{1}{3}\,\underset{\sim}{\sigma}\cdot\underset{\sim}{k}'\,\underset{\sim}{\sigma}\cdot\underset{\sim}{k}\right) \tag{31}$$

projects onto total angular momentum 3/2 .

One of the exciting possibilities of pion-nucleus scattering is that models of baryon structure in quark models[10-12] might be tested through a sufficiently careful implementation of the theory. Understanding of the one-pion exchange potential and meson exchange currents in nuclear physics has led to constraints on the size of the quark bag of the nucleon.[11] One might hope that similar statements about the size of the Δ_{33} bag [and other details of H' of Eq. (16)] might arise from applications of pion-scattering theory, because of the strong coupling between the pion and the Δ_{33}.

For example, in the bag model as applied to baryons, the three quarks fill a region of space of radius R, which is in turn determined by minimizing an energy functional, whose main contributions arise from (1) quark kinetic energy, which varies as 1/R, and (2) the bag energy which varies as R^3 and is interpreted physically as the source of pressure responsible for confinement. In the Stony Brook version[11] of the bag model there is an additional attractive term due to the pion coupling to the bag surface. The radius of the bag is usually taken to be the classical value, which is the location of the minimum of the energy functional. The general shape of the energy functional for the Stony Brook bag is shown in Fig. 3, and the minimum occurs for the nucleon at a radius of approximately 0.3 fm.

The coupling of the pion to the nucleon is determined by the principle of the conservation of axial vector current: inside the bag this current is carried by the quarks, and outside it is carried by the pion field. In order that the current be conserved, these two contributions must be continuous across the bag surface. In this fashion, one determines the pion-nucleon coupling constant as well as the dependence of the coupling on the pion momentum $\underset{\sim}{k}$, which specifies the form factor. For a bag of fixed radius R the form factor turns out to be[12]

$$v(k)=\frac{3j_1(kR)}{kR}\ , \tag{32}$$

where $j_1(kR)$ is a spherical Bessel function.

In a number of ways these bag models are too simple for the purposes of pion-nucleus physics. For one thing, the nucleon and Δ_{33} have different sizes in bag models. Since there is no overlap of the surfaces, and since the pion couples only at the surface, these

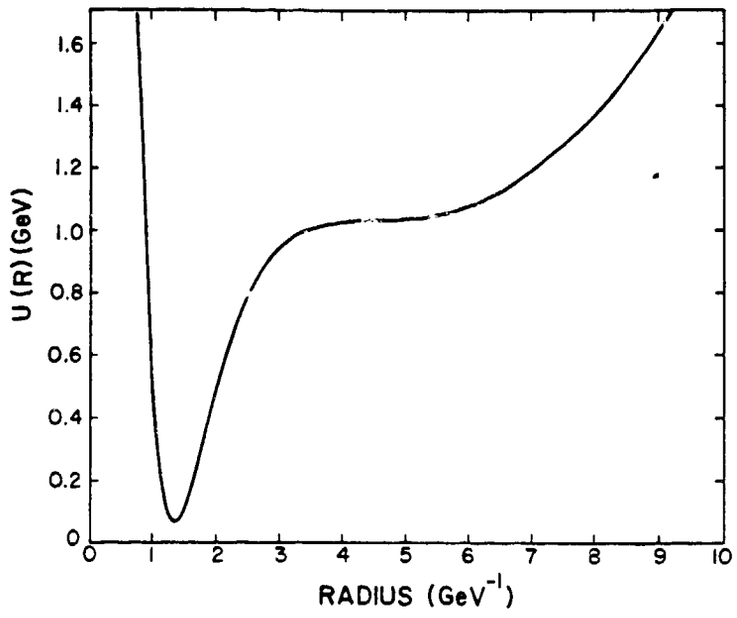

Fig. 3. Bag energy functional for a nucleon in the Stony Brook "little bag."

models, strictly interpreted, do not allow transitions between nucleons and Δ_{33}! For another thing the sharp surface of the bag introduces spurious high-momentum components in the form factor, which are undesirable due to the fact that pion couplings tend to emphasize high momenta.

As solutions to the theory become more sophisticated, these difficulties will disappear. I would now like to briefly describe one way that this would occur.[13] An obvious omission from the theory as described is quantum fluctuations of the surface around the classical radius. These fluctuations can be estimated under the assumption that the quarks move much more rapidly than the surface. In this case, the energy functional in Fig. 3 would play the role of the potential energy in a Schroedinger equation for the wave function $\psi(R)$ of the nuclear surface [$|\psi(R)|^2$ gives the probability that the bag surface is located at R],

$$\left[\frac{-\nabla^2}{2M^*} + U(R)\right]\psi(R) = E\psi(R) \quad , \tag{33}$$

which could be solved provided M^*, the effective mass of the surface zero-point motion, is known. In Ref. 13 this effective mass was estimated to be

$$M^* \approx 0.5\ M \tag{34}$$

under the assumption that only the quarks contribute to the vibrational energy and that the vibrational motion is homologous.

One of the consequences of this model is that the root mean square (rms) radius of the bag surface increases from 0.3 fm to about 0.7 fm. Estimates of the effect of a relativistic treatment of the surface[14] give a smaller rms radius of about 0.5 fm. One concludes from the relativistic model of surface zero-point motion that the form factor can be described by a cutoff mass Λ such that

$$v(k) = \frac{1}{k^2/\Lambda^2 + 1} \tag{35}$$

with $\Lambda \approx 1.4$ GeV/c for the πNN coupling and $\Lambda \approx 1.1$ GeV/c for the $\pi N\Delta$ coupling. Values this large are consistent with dispersion theory calculations.[15] Phenomenological treatments of pion scattering in field theoretical frameworks tend to give cutoffs of 765 to 980 MeV/c.[12,16] These smaller values presumably reflect the fact that nucleon recoil, which is normally omitted in the theoretical calculations, introduces additional cutoff factors. Recoil effects can be estimated by looking at the momentum dependence of the nucleon spinors and relativistic phase space. We estimate that an "intrinsic" cutoff of $\Lambda = 1.4$ GeV/c gets reduced by the recoil to $\Lambda = 1.03$ GeV/c, which is not so different from the larger phenomenological value.

The situation discussed here contrasts sharply with the more traditional ways of describing pion-nucleon scattering in terms of potentials. In these theories the cutoffs are much smaller, $\Lambda \approx 200$ MeV/c.[17] The reason for this is a combination of effects, the most severe of which is an intrinsic confusion of potential models between the energy dependence of the nucleon pole and the momentum dependence of the form factor.[16,18] Since the geometrical size of the nucleus as well as higher order terms of the optical potential are influenced by the range of the form factor, it is important at a quantitative level to go back to fundamental principles and describe the scattering in terms of the pion-nucleon couplings of Fig. 2, as we are doing.

Having chosen and discussed in detail a model for the underlying dynamics, let us now consider how to build up pion-nucleus scattering from it. Recall that we have chosen to assume that the nucleons are fixed at positions $\underset{\sim}{r}_1,\ldots,\underset{\sim}{r}_A$ as the pion multiply scatters through the nucleus. Finally, of course, it is necessary to average the nucleon positions over the wave function of the nucleus in order to calculate a cross section.

We will describe the Green's function for this model.[6] The rules of time-dependent perturbation theory for the calculation of G will not be derived. The specific form in which I state the rules may not be known to everybody, but the ideas for constructing time-

dependent amplitudes should be familiar from previous course work in quantum mechanics.[2]

We begin by describing the way to calculate the Green's function $G_{\alpha'\alpha}(t' - t; \underset{\sim}{r}_1, \underset{\sim}{r}_2, \ldots, \underset{\sim}{r}_A)$ for the pion, assuming that the nucleon sources are at fixed positions $\underset{\sim}{r}_1, \ldots, \underset{\sim}{r}_A$. Examples of diagrams for

$$G_{\underset{\sim}{k}'\underset{\sim}{k}}(t' - t; \underset{\sim}{r}, \ldots \underset{\sim}{r}_A) \tag{36}$$

are given in Fig. 4. The amplitude G is evaluated by summing all allowed diagrams, each of which is associated with a numerical value by definite rules to be described below. The allowed diagrams consist of A nucleon lines labeled by the spatial coordinates of the nucleons. These lines are directed by an arrow which points upward (the direction of increasing time). The diagrams each have two labeled times t' and t at which a directed pion line of quantum numbers k' terminates and a pion line of quantum numbers $\underset{\sim}{k}$ originates, respectively. These pion lines may connect to nucleons, as shown in Fig. 4(b) or may connect the times t' and t, as shown in Fig. 4(a).

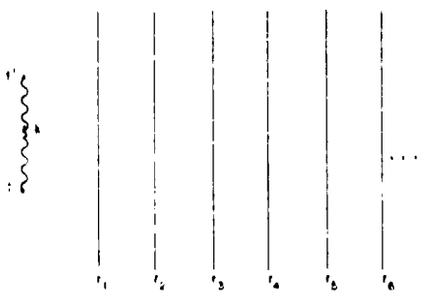

(a)

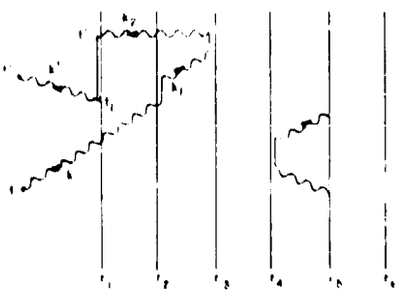

(b)

Fig. 4. Examples of diagrams contributing to the Green's function in Eq. (36). The labels for parts of the diagram are occasionally omitted to simplify the figure.

Otherwise, there may be any number of directed pion lines connecting the nucleon lines; pions may propagate either forward or backward in time. Each vertex at which a pion connects to a nucleon is assigned a distinct time label. Intermediate pion lines are labeled by quantum numbers $\underset{\sim}{k}''$, and nucleon line segments are labeled by i to distinguish between nucleons and Δ_{33} and to specify the spin and isospin quantum numbers.

Numerical values are associated with the diagrams as follows: (1) Each vertex at which a pion attaches to a nucleon is assigned a value given as a matrix element of the operators in Eqs. (17), (18), (20), (21), (24), and (25). (2) Meson line segments pointing upward are assigned the value

$$\frac{e^{-i\omega_k \Delta t}}{2\omega_k}\ \Theta(\Delta t) \tag{37}$$

and meson lines pointing downward

$$\frac{e^{-i\omega_k (-\Delta t)}}{2\omega_k}\ \Theta(-\Delta t)\ , \tag{38}$$

where Δt is counted in the direction of the arrow. (3) Intermediate nucleon line segments are assigned a value

$$\Theta(\Delta t) e^{-i\langle\varepsilon\rangle \Delta t}\ , \tag{39}$$

where $\langle\varepsilon\rangle$ is an average excitation energy[19] and intermediate Δ_{33}

$$\Theta(\Delta t) e^{-iM_\Delta \Delta t}\ . \tag{40}$$

(4) Sum over all intermediate labels. This sum includes the discrete quantum numbers of the pions, nucleons, and Δ_{33} as well as the intermediate pion momenta

$$\int \frac{d^3 k}{(2\pi)^3}$$

and the intermediate times

$$-i \int_{-\infty}^{\infty} dt\ . \tag{41}$$

Two useful identities are

$$e^{-i\omega_k(t'-t)}\theta(t'-t) = i\int_{-\infty}^{\infty}\frac{d\omega}{2\pi}\frac{e^{-i\omega(t'-t)}}{\omega-\omega_k+i\eta} \quad \text{and} \tag{42}$$

$$\frac{e^{i\omega_k(t'-t)}}{2\omega_k}\theta(t'-t) + \frac{e^{-i\omega_k(t-t')}}{2\omega_k}\theta(t-t')$$

$$= \frac{i}{2\pi}\int_{-\infty}^{\infty}d\omega\,\frac{e^{-i\omega(t'-t)}}{\omega^2-\omega_k^2+i\eta} \quad . \tag{43}$$

We have not said much about the term $u_{i'i}$ in Eq. (14). One should not forget to include it in evaluating the diagrams. It is needed because many of the interactions in higher order will have the effect of changing the nucleon and delta energies away from the values $\langle\varepsilon\rangle$ and m_Δ, which we have assumed them to have. Thus $u_{i'i}$ should be thought of as having whatever value is necessary to maintain these single-particle energies. It is analogous to the single-particle potential in low energy nuclear physics, which is usually added and subtracted from the many-body Hamiltonian before doing perturbation theory. The "added" piece establishes a set of basis states and the "subtracted" piece then cancels some important higher order terms and enables one to avoid double counting with the mesons in the nuclear force. The term $u_{i'i}$ here plays the role of the "subtracted" piece in conventional many-body physics.

By evaluating the diagrams in Fig. 4 according to the rules just described, the amplitude for a pion to scatter from a collection of sources fixed at $\underline{r}_1,\ldots,\underline{r}_A$ may be evaluated. To make the theory relevant to nuclei, we must take account of the fact that the nucleon positions are distributed throughout space as described by the nuclear wave function, ψ_N. The simplest realistic choice for ψ_N would be a Slater determinant of single-particle Hartree-Fock orbitals $\phi_i(r)$. Such wave functions are available from semimicroscopic[20(a)] and phenomenological[20(b)] models of the nucleon-nucleus interaction. For closed shell nuclei, the appropriate wave function may be written

$$\langle\underline{r}_1,\ldots,\underline{r}_i|\psi_N\rangle = \mathcal{A}\prod_{i=1}^{A}\phi_i(r_i) \quad . \tag{44}$$

where $\mathcal{A}$ is the antisymmetrization operator. A more realistic choice would include a modification of Eq. (44) by two-body correlations represented by $f(r_{ij})$

$$\langle\underline{r}_1,\ldots,\underline{r}|\psi_N\rangle = \mathcal{A}\prod_{i<j}f(r_{ij})\prod_k\phi_k(r_k) \quad . \tag{45}$$

An explicit expression for $f(r_{ij})$ and $\phi_k(r_k)$ might be obtained from a variational calculation applied to a finite nucleus.

In order to incorporate the nuclear wave functions one may continue to use diagrammatic analysis. We consider here only the wave function in Eq. (44). The matrix element we want is

$$G_{k'k}(t' - t) = \langle\psi_N|\, G_{k'k}(t' - t;\, \underset{\sim}{r}_1,\ldots,\underset{\sim}{r}_A)|\psi_N\rangle \,/\, \langle\psi_N|\psi_N\rangle \quad . \tag{46}$$

This expectation value is a straightforward modification to Fig. 4. Each initial and final nucleon line is labeled by one of the quantum numbers of the occupied orbitals, so that each diagram is multiplied by the product

$$\prod_i \int d^3r_i\; \phi^*_{A_i}(r_i)\phi_{B_i}(r_i) \quad . \tag{47}$$

It is also necessary to determine the sign of the diagram, which has its origin in the Pauli principle through the antisymmetrization operator in Eq. (44). Because the wave function must change sign upon interchange of the state labels of any two particles, the sign of the diagram is

$$(-)^{N_x} \quad , \tag{48}$$

where N_x is the number of interchanges of initial- and final-state labels needed to bring the order of labels to a standard sequence.

It remains now to identify the optical potential U. We saw in the discussion of Fig. 1 that U is identified as the amplitude for the propagation of the excited medium. Therefore, to determine U we must isolate this amplitude from our diagrams. We show in Fig. 5(a) one of the terms contributing to Eq. (46) with its state labels given explicitly. To identify U we want to make this picture resemble one of the histories in Fig. 1. In order to do this, we will eliminate the superfluous nucleon lines and the unlinked terms, i.e., pieces that correspond to a spontaneous medium excitation uncorrelated with the initial and final pion [e.g., the excitation connecting lines D and E in Fig. 5(a)]. The procedure that accomplishes this change of appearance is simply: connect the initial and final nucleon lines having the same state labels. This does not change the value of the diagram, but it immediately simplifies the pictures because the noninteracting lines [e.g., line F in Fig. 5(a)] do not have to be drawn. The change of notation also simplifies keeping track of the Pauli principle. The sign rule in Eq. (48) becomes

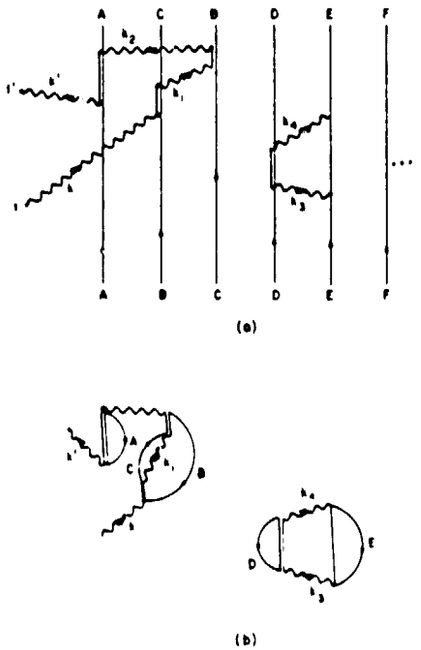

Fig. 5. Two equivalent notations for a term resulting from averaging the diagram in Fig. 4(b) over a product wave function for the nucleons.

$$(-)^{\Sigma(\ell+c)} \quad , \tag{49}$$

where $\Sigma(\ell + c)$ is the sum of all the closed nucleon loops and labeled "hole" lines. The validity of the rule in Eq. (49) may be verified after a bit of thought. The diagram in Fig. 5(a) is redrawn in the new notation in Fig. 5(b).

One should notice a very useful consequence of the sign rule in Eq. (49). When evaluating diagrams in the new notation it is permissible to sum the hole lines over <u>all</u> normally occupied state labels without restriction. The reason one does not have to worry about overcounting is that the sign rule assures that terms violating the Pauli principle will cancel in pairs. A further consequence is that the unlinked terms such as the vacuum fluctuation in Fig. 5 may be regarded as occurring equivalently along with all linked diagrams (i.e., all terms linked to the times t′ and t). They are therefore a common factor (they can be shown to be a pure phase) and may be ignored. However, once they are omitted, those that remain may contain legitimate pieces that appear to violate the Pauli principle.

We have now finished the derivation of our expansion, and it may be compared term by term with any of the histories in Fig. 1 to isolate the amplitude U for propagation of the pion-excited medium. A

few of the terms that contribute to $\langle \underset{\sim}{k}' | U | \underset{\sim}{k} \rangle$ are shown in Fig. 6. When the arrow on the final momentum $\underset{\sim}{k}'$ leaves the diagram as in Fig. 6(a), we shall call the diagram uncrossed. A given uncrossed term "n" will be denoted by

$$\text{uncrossed} = \langle \underset{\sim}{k}' | B_n(t' - t) | \underset{\sim}{k} \rangle \quad . \tag{50}$$

All terms also occur in the form of crossed pieces as in Fig. 6(b). The expressions for the crossed piece corresponding to "n" are easily obtained from the uncrossed by our rules for evaluating diagrams,

$$\text{crossed} = \langle -\underset{\sim}{k} | B_n(t - t') | -\underset{\sim}{k}' \rangle \quad , \tag{51}$$

so that in general $F(\underset{\sim}{k}', \underset{\sim}{k}; t' - t)$ is given by

$$F(\underset{\sim}{k}', \underset{\sim}{k}; t' - t) = \sum_n \left[\langle \underset{\sim}{k}' | B_n(t' - t) | \underset{\sim}{k} \rangle + \langle -\underset{\sim}{k} | B_n(t - t') | -\underset{\sim}{k}' \rangle \right] \quad . \tag{52}$$

From Eq. (12) we find

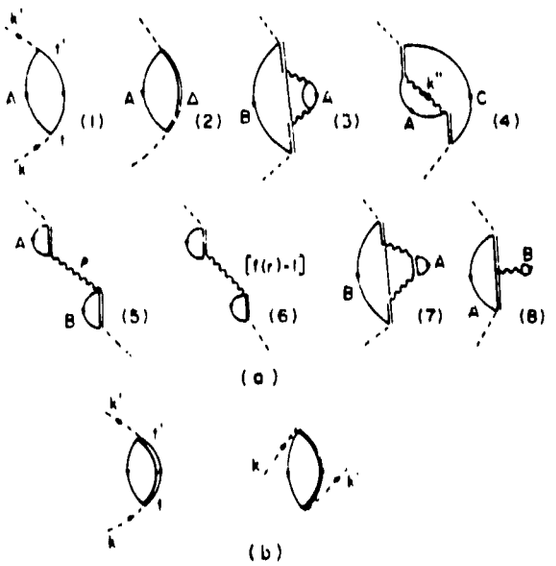

Fig. 6. Terms which contribute to the amplitude for propagation of the pion-excited medium. The dashed lines represent the initial and final pion state and do not contribute propagator factors to the value of the diagram. (a) These are uncrossed contributions. (b) Each uncrossed term has an associated crossed term which must be included. No attempt has been made to give an exhaustive list.

$$\langle \underset{\sim}{k}' | U(\omega) | \underset{\sim}{k} \rangle = \sum_n \left[\langle \underset{\sim}{k}' | B_n(\omega) | \underset{\sim}{k} \rangle + \langle -\underset{\sim}{k} | B_n(-\omega) | -\underset{\sim}{k}' \rangle \right] \quad . \tag{53}$$

Note that our optical potential U is crossing symmetric, i.e.,

$$\langle \underset{\sim}{k}' | U(\omega) | \underset{\sim}{k} \rangle = \langle -\underset{\sim}{k} | U(-\omega) | -\underset{\sim}{k}' \rangle \quad . \tag{54}$$

This symmetry property arises naturally in the theory and is easily preserved order by order in the evaluation of U. In some other theories[21-23] this property is established as the result of the solution of integral equations. The simplicity of U as evidenced in part by this symmetry property is lost when one formulates the theory in terms of time-ordered diagrams, but as shown in Ref. 2, this symmetry could be recovered by complicated diagrammatic resummations.

Equation (53) is our main theoretical result. Expressions for optical potentials have also been obtained for field theoretical models by other investigators (see, for example, Ref. 24).

In the remainder of my lectures, I want to present a systematic application of the theory to experiment. The idea is to learn as much as possible about the fundamental couplings and nuclear dynamics. In order to enhance the possibility for doing this, we shall find it desirable to extend the theory to describe charge exchange, exploiting the isospin symmetry of the underlying interactions. We shall make this extension in the next lecture.

II. Applications

Now I would like to describe applications of the basic theory. The first application is elastic scattering and the second is charge exchange to isobaric analog states.

Let me first summarize the main results of the first lecture. I showed there how to derive the optical potential U for elastic pion-nucleus scattering from an underlying field theoretical model. Some of the important properties of this theory are:

(1) U is given through a well-defined cluster expansion. In order to evaluate U one must know the nuclear single-particle orbitals and the values of the meson absorption and emission amplitudes given in Fig. 1.

(2) U must be embedded in the Klein-Gordon equation

$$(-\nabla^2 + m_\pi^2 + U)\psi = \omega^2 \psi \quad . \tag{55}$$

(3) U and the scattering T matrix are crossing-symmetric in principle; this property is preserved order by order in our cluster expansion.

(4) Multipion intermediate states are intrinsically built into the theory.

(5) Short-range pion-nucleon form factors (of a range parameter $\Lambda \approx 1$ GeV) are proper to use.

The derivation of our results relied on the static approximation. This is an unnecessary restriction and must be relaxed in order to compare the results to experiment. The properties listed above will survive the extension of the theory. In fact, the extended theory may be cast into a form very similar to that given in Lecture I, but the rules for evaluating the diagrams are somewhat altered. We shall next make some heuristic modifications to take account of the recoil and binding of the nucleons, but we will not discuss systematically the required extensions. A complete discussion of this is given in Ref. 25.

Let us begin by examining the first-order optical potential, $U^{(1)}$. This is represented diagrammatically in Fig. 7. The boxes are the pion-nucleon scattering amplitude. We assume that the many terms in the theory contributing to these boxes have been summed and that the result is known. This amplitude has not been obtained from the theory in a completely satisfactory manner, but there are derivations of it in a purely Chew-Low model[16] and in the cloudy-bag model,[12] which give similar extensions of the amplitude off shell. One of the

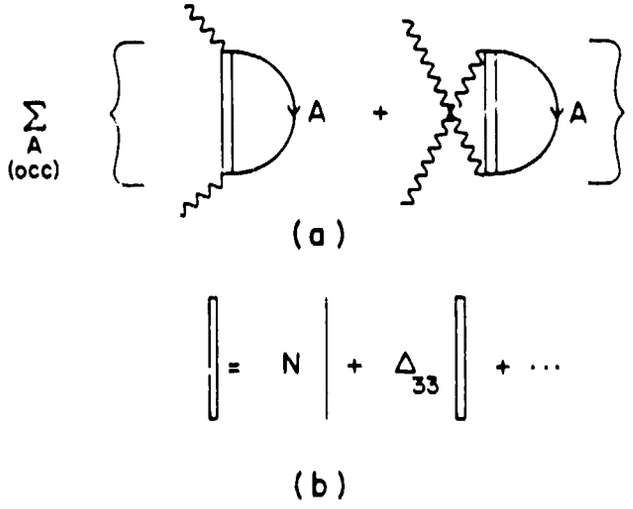

Fig. 7. Lowest order optical potential. (a) The general form for $U^{(1)}$ in terms of the pion-nucleon scattering amplitude. (b) Prominent terms occurring in the $\ell = 1$ partial wave of the pion-nucleon system.

very interesting unresolved[26] questions is to what extent the resonance in the (3,3) channel is Chew-Low (multiple emission and absorption of the pion) and to what extent elementary Δ_{33}. In the absence of a definite answer to these questions, we take guidance from Ref. 16, which expresses the off-shell pion-nucleon amplitude $T_{\pi N}$ in a separable form,

$$\langle \underset{\sim}{\kappa}' | T_{\pi N}(\omega) | \underset{\sim}{\kappa} \rangle = \sum_{\alpha} P_{\alpha} v(\underset{\sim}{\kappa}') \lambda_{\alpha}(\omega) v(\kappa) \quad , \tag{56}$$

where $\underset{\sim}{\kappa}$ is the pion-nucleon relative momentum, P_{α} is a projection operator onto the partial-wave channels [see, for example, Eqs. (30) and (31)], $v(\kappa)$ is the pion-nucleon form factor and $\lambda_{\alpha}(\omega)$ is an energy-dependent factor which can be related to the experimental phase shifts in channel α. Figure 7(a) expresses how the amplitude in Eq. (56) is to be averaged over nuclear wave functions to obtain the optical potential.

Before recording the result of evaluating Fig. 7, I want to make a few remarks on the inclusion of proper kinematics, i.e., the extension of the lowest order optical potential beyond the static approximation. Consider nonrelativistic kinematics for simplicity and write the pion-nucleon T matrix in an arbitrary frame of reference as

$$\langle \underset{\sim}{k}' \underset{\sim}{p}' | T_{\pi N}(E) | \underset{\sim}{k} \underset{\sim}{p} \rangle \quad , \tag{57}$$

where $\underset{\sim}{k}(\underset{\sim}{p})$ is the pion (nucleon) momentum and E the incident energy

$$E = m + M + \frac{k^2}{2m} + \frac{p^2}{2M} \quad . \tag{58}$$

Translational invariance tells us how to relate the matrix element in Eq. (57) to a matrix element of T_{cm}, the T matrix evaluated in the pion-nucleon center-of-mass frame of reference. The result is

$$\langle \underset{\sim}{k}' \underset{\sim}{p}' | T_{\pi N}(E) | \underset{\sim}{k} \underset{\sim}{p} \rangle = \langle \underset{\sim}{\kappa}' | T_{cm}(E_{cm}) | \underset{\sim}{\kappa} \rangle \tag{59}$$

where

$$E_{cm} = E - \frac{P^2}{2(M + m)} \tag{60}$$

with $\underset{\sim}{P}$ the total momentum

$$\underset{\sim}{P} = \underset{\sim}{k} + \underset{\sim}{p} \tag{61}$$

and $\underset{\sim}{\kappa}$ the relative momentum

$$\underset{\sim}{\kappa} = \underset{\sim}{k} - \frac{m\underset{\sim}{P}}{M + m} \quad . \tag{62}$$

In practice, of course, these corrections must be made relativistically. By including the nucleon momentum in Eq. (62) one mixes s waves and p waves; this is generally referred to as making an "angle transform." The energy correction in Eq. (60) is very important near resonance, but at low energy where the ω dependence in Eq. (56) is weak, one often assumes that the struck nucleon was at rest in evaluating this term.

A few of the important second-order terms that must be included in the theory were shown in Fig. 6. The terms which have been most extensively studied in pion scattering are Fig. 6(a3), which is a manifestation of "true absorption" in elastic scattering; Fig. 6(a4), which is the Pauli correlation; and Fig. 6(a5) and (a6), which are, respectively, corrections for short-range correlations arising from the ρ meson and the short-range repulsion in the nucleon-nucleon interaction. The latter effect is included by introducing the short-range correlation function $f(r)$ in Eq. (45). A systematic cluster expansion of U in terms of the wave function in Eq. (45) is possible, in which case $f(r)$ would build up the radial distribution function between nucleon pairs. This function is sketched in Fig. 8. The vanishing of this function for small r is the effect of the repulsive core in the nucleon-nucleon interaction. The correlations give rise to what is sometimes called the "Lorentz-Lorenz Ericson-Ericson" (LLEE) effect.[27] The evaluation of these terms is straightforward in terms of the rules that we have given, and we will postpone discussion of this to Lecture III.

Next I want to discuss the comparison of the theory to low-energy pion elastic scattering. The standard theory for this is the theory of K. Stricker, H. McManus, and J. Carr (SMC).[28] The theory originated in the series of papers in Refs. 27-31. The form of the theory fits very nicely into the framework given in Lecture I. In Ref. 28, U is given explicitly as

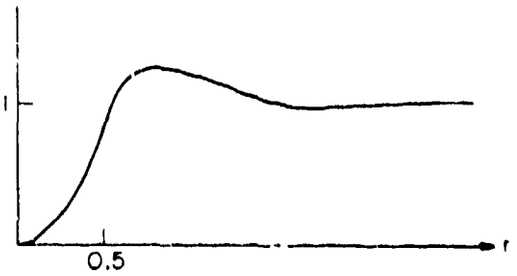

Fig. 8. Pair distribution function for nucleons.

$$U = -4\pi[b(r) + B(r)] + 4\pi\underset{\sim}{\nabla} \cdot \{L(r)[c(r) + C(r)]\}\underset{\sim}{\nabla}$$

$$-4\pi[\frac{p_1 - 1}{2} \nabla^2 c(r) + \frac{p_2 - 1}{2} \nabla^2 C(r)] \quad , \tag{63}$$

where

$$b(r) = p_1[\bar{b}_0\rho(r) - \varepsilon_\pi b_1 \Delta\rho(r)] \quad , \tag{64}$$

$$\bar{b}_0 = b_0 - (3/2\pi)\, 1.4\, (b_0^2 + b_1^2) \quad , \tag{65}$$

$$c(r) = p_1^{-1}[c_0\rho(r) - \varepsilon_\pi c_1 \Delta\rho(r)] \quad , \tag{66}$$

$$B(r) = p_2 B_0 \rho^2(r) \quad , \tag{67}$$

$$L(r) = \{1 - (4\pi/3)\lambda[c(r) + C(r)]\} \quad , \tag{68}$$

$$\Delta\rho(r) = \rho_n(r) - \rho_p(r) \quad , \tag{69}$$

$$p_1 = 1 + \omega/M \; , \; p_2 = 1 + \omega/2M \quad , \tag{70}$$

and where ε_π is the pion charge. The coefficients b_0, b_1, C_0, and C_1 describe the pion-nucleon scattering amplitude $f_{\pi N}$.

$$f_{\pi N} = b_0 + b_1 \underset{\sim}{\phi} \cdot \underset{\sim}{\tau} + (c_0 + c_1 \underset{\sim}{\phi} \cdot \underset{\sim}{\tau})\underset{\sim}{k}' \cdot \underset{\sim}{k} \quad , \tag{71}$$

where $\underset{\sim}{\phi}$ is the pion and $\underset{\sim}{\tau}$ the nucleon isospin operators. The correction to b_0 in Eq. (65) is the effect of the Pauli principle in s waves. The quantities B(r) and C(r) are second-order effects describing the true absorption of pions in s and p waves, respectively. The quantity L(r) describes the LLEE effect; λ is taken as an adjustable parameter and is interpreted in Refs. 32 and 33 as the combined effect of the ρ meson and nuclear short- and long-range correlations. The quantities p_1 and p_2 are a measure of the importance of nucleon recoil, and therefore the importance of the angle transformation. If p_1 and p_2 are set equal to 1, then the static limit results.

The importance of the SMC potential is that it gives a systematic reproduction of low-energy elastic-scattering data for pion kinetic energy $T_\pi \lesssim 50$ MeV. The same parameters describe the level

shifts and widths of π^- in atomic orbits. See Ref. 7 for a detailed comparison of the parameters to the theory. Suffice it to say here that the experiment and theory are consistent in most respects. Perhaps the most significant feature of low-energy scattering is the relative weakness of U. This comes about in a rather intricate fashion. Without second-order corrections, it pays for the pion wave function to develop high-momentum components to enhance the attraction in the p-wave piece of the optical potential, which then becomes anomalously strong at low energies. The effect of the correlations is to weaken the p-wave piece of the potential so that at normal densities this anomalous behavior does not occur.[34] As a result, the pion penetrates farther into the nucleus and is more strongly influenced by the interesting high-density region. The data are not understood even qualitatively without the second-order terms. The sensitivity of the scattering to individual terms was calculated in Ref. 31 and the results shown in Fig. 9. The experimental points are from Ref. 39 and are shown to establish a scale. The more recent fits to the data are those given in Ref. 28.

Next let me consider pion scattering near the (3,3) resonance. Here the physics is qualitatively different. For one thing, the pion-nucleon scattering amplitude is much stronger, meaning that the pion penetrates less deeply into the nucleus and that the cross sections have a strong diffractive character. This has the consequence that one can understand semiquantitatively a large variety of scattering data in relatively simple terms. (Some of these simple results are mentioned in Lecture III.) On the other hand, the rapid variation of the amplitude with energy means that the details of the scattering are sensitive to the way the nucleon and Δ_{33} energies are handled in the evaluation of the optical potential.

Let us begin the discussion of the resonance energy by examining more carefully the energy in the evaluation of lowest order potential. Consider for simplicity the uncrossed term in Fig. 7(a). The rapid energy variation occurs in $\ell = 1$ partial wave for the Δ_{33} contribution to the amplitude [that the Δ_{33} resonance occurs in $\ell = 1$ is evident from Eq. (31)]. In the static theory the amplitude has the form

$$T_{33} = V \frac{1}{\omega - m_\Delta + i\Gamma(\omega)/2} V \quad , \tag{72}$$

where V represents the $\pi N\Delta$ vertex and ω is the incident energy. In going beyond the static theory one must be sure to include in ω the energy of the struck nucleon "A" in addition to the energy of the incident pion

$$\omega + \omega_\pi + E_A \tag{73}$$

and similarly replace the mass of the Δ_{33} by its true energy

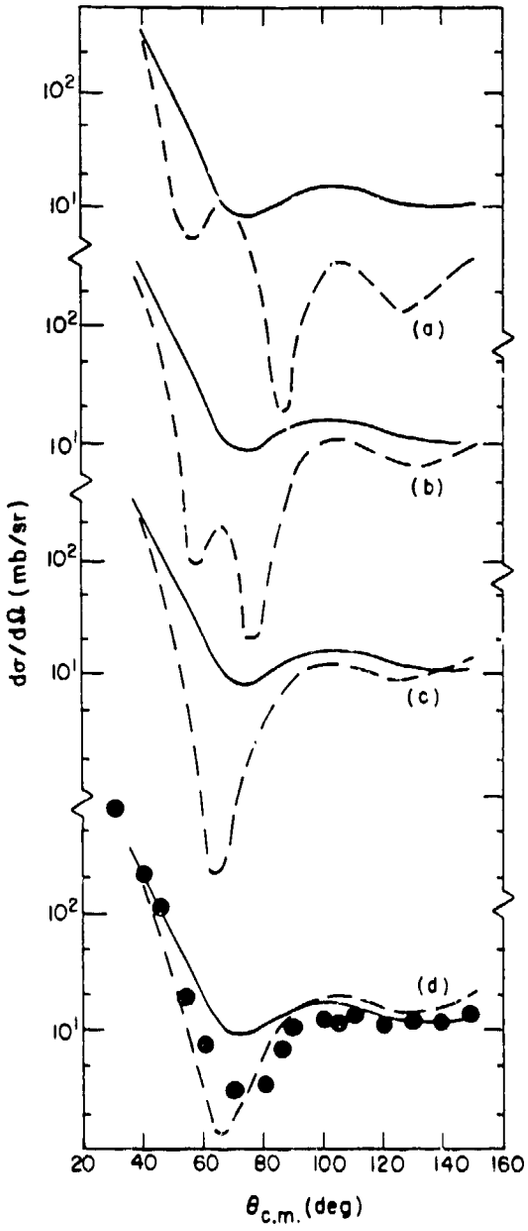

Fig. 9. Demonstration of the importance of the various terms in Eq. (63) for low-energy pion scattering (T_π = 50 MeV) on ^{208}Pb. The solid curve represents the full calculation and the circles are the experiment, taken from Ref. 39. The dashed lines are: (a), the Kisslinger potential only; (b), the result of (a) plus the angle transformation; (c), the result of (b) plus s-wave true absorption; (d), the result of (c) plus the Pauli correction.

$$m_\Delta + H_\Delta = \frac{p^2}{2(M+m)} + U_\Delta + m_\Delta \quad , \tag{74}$$

where U_Δ is the interaction potential energy of the Δ_{33} with the nucleus and $\underset{\sim}{P}$ the momentum of the Δ_{33}. The Δ_{33} kinetic energy is, of course, the same as the correction previously discussed in Eq. (60). One does not currently have a reliable theory of U_Δ, but as a first guess one might take it to be the same as the nucleon-nucleus potential, and describe the presumably small corrections to this perturbatively in the second-order optical potential.

A phenomenology which addresses the modifications just discussed is the isobar-hole model of Ref. 4. Although this model is based on traditional multiple-scattering theory and is not solved in an optical-model framework, it is useful to examine the results to obtain an orientation to scattering in the resonance region. Their model of H_Δ includes a correction ΔU_Δ, which is added to Eq. (74)

$$\Delta U_\Delta = \text{Pauli correction} + \text{spin orbit} + W_0 \rho(r) \quad , \tag{75}$$

and which describes the energy of the Δ_{33} relative to that of a nucleon. The parameter W_0 and those characterizing the single-particle spin-orbit force are determined by adjusting them to obtain a best fit to elastic-scattering data. The results they obtain for W_0 are shown in Fig. 10. A positive $\mathrm{Re}W_0$ indicates that the isobar is less strongly bound to the nucleus than a nucleon and the negative $\mathrm{Im}W_0$ indicates that the isobar width is increased in the medium due to interactions with other nucleons.

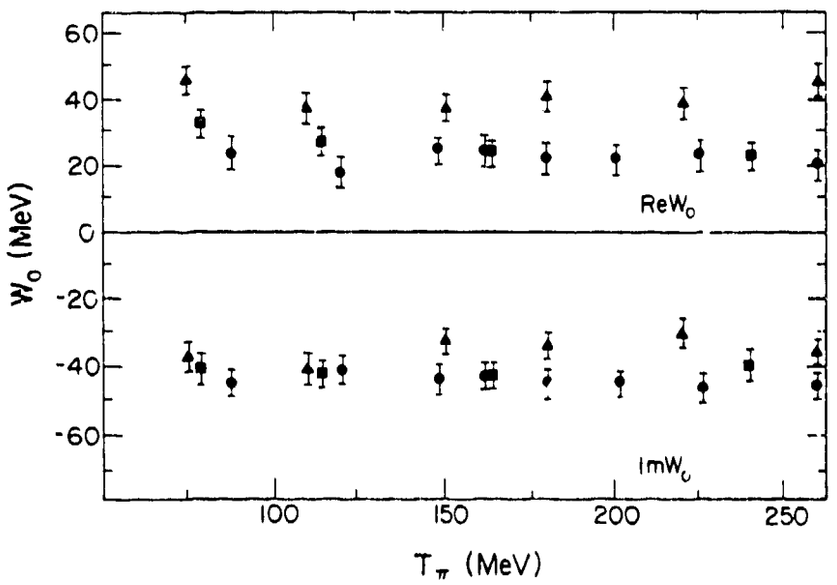

Fig. 10. Strength of the isobar spreading potential W_0 of Eq. (75). The results are from Ref. 4a. The triangles come from an analysis of ^{4}He; the squares, ^{16}O; and the circles, ^{12}C.

Let us now estimate the importance of the energy shifts that occur in the modifications of Eq. (72). The effect of the kinetic energy operator was examined in Ref. 40. There it is shown that if the V's in Eq. (72) are neglected, then for a peripheral partial wave ℓ, the kinetic energy operator may be replaced by the average given by

$$\frac{\langle P^2 \rangle}{2(M+m)} = \frac{k_\pi^2}{2(M+m)} + \frac{\beta^2}{2(M+m)} + \frac{2\beta(\kappa_\pi^2 + \beta^2)^{1/2}}{2(M+m)\ell} \quad , \tag{76}$$

where k_π is the incident pion momentum and where β is the rate of fall-off of the nuclear wave-function in the nuclear surface

$$\psi(r) \sim e^{-\beta r}/r \quad . \tag{77}$$

If we evaluate for the correction term for ^{16}O, taking $\ell = k_\pi R$, $R = 3.5$ fm, and $k_\pi = 1.4$ fm^{-1}, corresponding to the resonance energy, then

$$\frac{\langle P^2 \rangle}{2(M+m)} = \frac{k_\pi^2}{2(M+m)} + 25.2 \text{ MeV} \quad . \tag{78}$$

What about the potential energies? The average energy of a bound nucleon in ^{16}O can be estimated from Hartree-Fock theory. We find from Ref. 41 that

$$\langle E_A \rangle = \frac{\Sigma(2\ell+1)E_{n\ell}}{\Sigma(2\ell+1)} \approx -22 \text{ MeV} \quad . \tag{79}$$

On the other hand, we may estimate $\langle U_\Delta \rangle$ by noting that the scattering takes place in the nucleus in a region specified by the overlap of the nuclear density and the square of the pion wave function, so

$$\langle U_\Delta \rangle = \frac{\int U_\Delta(r)\, |\Psi_\pi(r)|^2\, \rho(r) d\tau}{\int |\Psi_\pi|^2\, \rho(r) d\tau} \tag{80}$$

We have evaluated this[42] for ^{16}O and find that $\langle U_\Delta \rangle \approx -24$ MeV for resonance-energy pions. The energy dependence of $\langle U_\Delta \rangle$ is shown in Fig. 11. Summing the contributions in Eqs. (78), (79), and (80), we find

$$\text{Net energy shift} = -23 \text{ MeV} \quad . \tag{81}$$

This is a significant effect in the denominator of Eq. (72), given

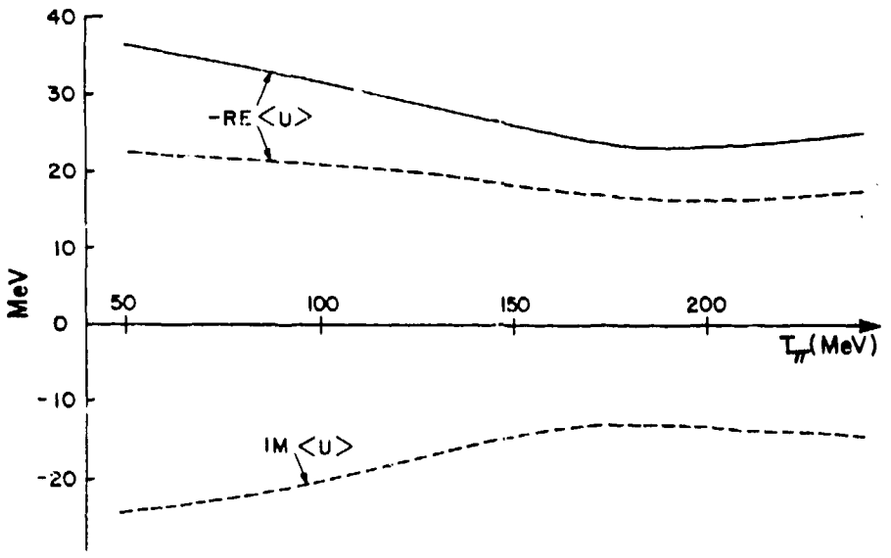

Fig. 11. Energy dependence of $\langle U_\Delta \rangle$ in MeV. The dashed lines include the effect of the spreading potential taken from the isobar-doorway model.

that $\Gamma/2 = 55$ MeV. Phenomenological studies[43] have shown that elastic-scattering data can be systematically reproduced throughout the resonance region in terms of an optical potential similar to that in Eq. (63), provided the lowest order optical potential is evaluated at an energy shifted downward by 25-30 MeV, which is very close to the estimate in Eq. (81).

It is worth noting that the width in Eq. (72) is also modified by binding energy and recoil considerations,[4,44] and that in general one must expect phenomenological energy shifts to be complex.

In order to test any given dynamical theory it is of course necessary to calculate the energy shift rather than treat it as a phenomenological parameter. This is especially true of theories which address only elastic scattering, because the dynamical effects that are included in the second-order optical potential affect the theory in much the same way as the energy shifts arising from binding energy and recoil corrections. Progress is being made in building a theory in which these effects are actually calculated,[42,45] but I will not further discuss this line of research here.

Let me now discuss the extension of these ideas to include pion charge exchange to isobaric analog states, exploiting the (approximate) isospin symmetry of the strong interaction. If we define the total isospin operator,

$$\underline{T} = \underline{T}_N + \underline{t} \quad , \tag{82}$$

where $\underline{t}$ is the pion isospin operator and $\underline{T}_N$ is the nuclear isospin operator,

$$\underline{T}_N = \frac{1}{2} \sum_{i=1}^{A} \underline{\tau}_i \quad , \tag{83}$$

then the isospin invariance of the interaction is expressed by stating

$$[H, \underline{T}] = 0 \quad . \tag{84}$$

This is true, of course, only to the extent that we omit the Coulomb force and other presumably small isospin-breaking terms. If we assume Eq. (84) to be true, then we may express the scattering amplitude F in the space spanned by the isospin components of the nuclear ground state and nuclear single- and double-isobaric analog states explicitly and generally in terms of $\underline{t}$ as

$$\hat{F} = F_0 + F_1 \, \underline{t} \cdot \underline{T}_N + F_2 (\underline{t} \cdot \underline{T}_N)^2 \quad , \tag{85}$$

noting that this operator must also commute with $\underline{T}$,

$$[\hat{F}, \underline{T}] = 0 \quad . \tag{86}$$

Since we want to be able to calculate $\hat{F}$ in an optical model theory, we must choose U to have the same form as F in Eq. (85),

$$\hat{U} = U_0 + U_1 \, \underline{t} \cdot \underline{T}_N + U_2 \, (\underline{t} \cdot \underline{T}_N)^2 \quad . \tag{87}$$

The term U_0 is referred to as the isoscalar, U_1 as the isovector, and U_2 as the isotensor potential. Use of an optical potential of this form has been previously advocated in Refs. 27 and 46. An alternative approach to the study of charge exchange is the distorted wave-impulse approximation.[47,48]

In physical terms, the extension of the theory to include isobaric analog states means the following. For nuclei with a neutron excess, we may represent the ground state as in Fig. 12. In single-charge-exchange scattering to the isobaric analog state any one of the N-Z excess neutrons can be converted to a proton in the same space-spin orbit. The resulting collective excitation is the isobaric analog transition. In double-charge exchange the same thing may happen to two of the excess neutrons. Mathematically these two states are represented as, respectively

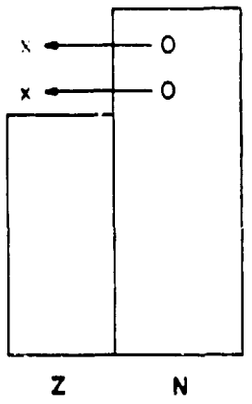

Fig. 12. Representation of the ground state of a nucleus having a neutron excess. The single (double) isobaric analog state is a collective excitation in which one (two) neutron(s) at a time are converted to protons with the same space-spin quantum numbers.

$$|A^{(1)}\rangle = T_N^+|gs\rangle \,/\, \langle gs|T_N T_N^+|gs\rangle \quad \text{and} \tag{88}$$

$$|A^{(2)}\rangle = (T_N^+)^2|gs\rangle \,/\, \langle gs|T_N^2 (T_N^-)^2|gs\rangle \quad , \tag{89}$$

where T_N^+ is the nuclear isospin-raising operator. (Isospin-breaking effects may be formally taken into account by replacing T_N with the "analog spin" operator W. See Ref. 49.) Because the three processes, namely elastic scattering,

$$|\pi^\pm gs\rangle \rightarrow |\pi^\pm gs\rangle \quad ; \tag{90}$$

single-charge exchange,

$$|\pi^+ gs\rangle \rightarrow |\pi^0 A^{(1)}\rangle \quad ; \tag{91}$$

and double-charge exchange,

$$|\pi^+ gs\rangle \rightarrow |\pi^- A^{(2)}\rangle \quad , \tag{92}$$

are intimately connected by the symmetry of isospin invariance, we expect to find a relatively simple theoretical description which will

tell us directly about the isospin dependence of the nuclear response as represented by the optical potential.

We will now discuss how the results in Lecture I may be extended to charge exchange, following Refs. 50 and 51. We will use the ideas of the spectator expansion of Ref. 52. The spectator expansion shows how to systematically express the optical potential U in terms of the T matrix for the scattering of a projectile from 1,2,...,N nucleons. In Ref. 52 it was used to give U for elastic scattering, but we shall extend it to calculate the optical potential for the combined theory of elastic and charge-exchange scattering.

Begin by defining $A^{(n)}(i)$ as the sum of all diagrams which have n hole lines and which contribute to the scattering amplitude of a pion of charge i. This quantity is specified by the rules of Lecture I. Also define $\langle\hat{U}^{(n)}\rangle^i$ as the matrix element of the nth-order optical-potential piece of Eq. (87) corresponding to the scattering of a pion of charge i from the ground state. Thus, the brackets $\langle\ \rangle^i$ mean, for example,

$$\langle\hat{U}^{(n)}\rangle^i \equiv \langle\pi^+ gs|\hat{U}^{(n)}|\pi^+ gs\rangle \quad . \tag{93}$$

The spectator expansion says simply

$$\begin{aligned}
\langle\hat{U}^{(1)}\rangle^i &= A^{(1)}(i) \quad , \\
\langle\hat{U}^{(2)}\rangle^i &= A^{(2)}(i) - \langle\hat{U}^{(1)}G_0\hat{U}^{(1)}\rangle^i \quad , \\
\langle\hat{U}^{(3)}\rangle^i &= A^{(3)}(i) - \langle\hat{U}^{(2)}G_0\hat{U}^{(1)}\rangle^i - \langle\hat{U}^{(1)}G_0\hat{U}^{(2)}\rangle^i \\
&\quad - \langle\hat{U}^{(1)}G_0\hat{U}^{(1)}G_0\hat{U}^{(1)}\rangle^i \quad ,
\end{aligned} \tag{94}$$

and so on. The series is defined so that the matrix element $\langle\hat{F}\rangle^i$ of Eq. (85) can be calculated by solving the equation

$$\hat{F} = \hat{U} + \hat{U}G_0\hat{F} \tag{95}$$

with the requirement that $\langle\hat{F}^{(n)}\rangle^i = A^{(n)}(i)$. To obtain $\hat{U}^{(n)}$ in the operator form of Eq. (87) from $\langle\hat{U}^{(n)}\rangle^i$ of Eq. (94) we use isospin invariance. It is straightforward to invert[53] Eq. (87) to obtain

$$U_2 = \frac{1}{T(2T-1)}\left(\langle\hat{U}\rangle^+ + \langle\hat{U}\rangle^- - 2\langle\hat{U}\rangle^0\right) \quad ,$$

$$U_1 = \frac{1}{T}\left(\langle\hat{U}\rangle^0 - \langle\hat{U}\rangle^+\right) + TU_2 \quad , \text{ and} \tag{96}$$

$$U_0 = \langle\hat{U}\rangle^0 - TU_2 \quad ,$$

where T is the ground-state nuclear isospin.

By using this procedure we are led to an optical-model theory which is similar in form to that of SMC, but which now contains explicit dependence on the isospin operators $\underline{t}$ and $\underline{T}_N$. I will now state the overall form of the optical-model theory.[51] The theory employs a special form for $\hat{U}^{(2)}$ which was derived in Ref. 50 and given below; this result will be discussed in greater detail in Lecture III. The optical model is

$$\hat{U} = \nabla\cdot[\hat{\xi}(r) + \Delta\hat{\xi}(r)]\nabla - k^2[\hat{\xi}(r) + \Delta\hat{\xi}(r)]$$

$$- \frac{1}{2}(p_1 - 1)\nabla^2\hat{\xi} - \frac{1}{2}(p_2 - 1)\nabla^2\Delta\hat{\xi} \quad , \tag{97}$$

where $\hat{\xi}$ and $\hat{\bar{\xi}}$ represent the lowest order optical potential and have the form

$$\hat{\xi} = \xi_0 + \underline{t}\cdot\underline{T}_N\xi_1 \quad , \tag{98}$$

and where $\Delta\hat{\xi}$ and $\Delta\hat{\bar{\xi}}$ represent the second-order optical potential and have the form

$$\Delta\hat{\xi} = \Delta\xi_0 + \Delta\xi_1\underline{t}\cdot\underline{T}_N + \Delta\xi_2(\underline{t}\cdot\underline{T}_N)^2 \quad . \tag{99}$$

Note that the lowest order optical potential has no isotensor term, because two nucleons must be struck in order to charge exchange twice.

We find it convenient to express ξ and $\Delta\xi$ in terms of a set of parameters $\lambda_i^{(1)}$ and $\lambda_i^{(2)}$, respectively. For the lowest order potential

$$\xi_0 = \lambda_0^{(1)}\rho(r) \quad \text{and} \tag{100}$$

$$\xi_1 = \frac{\lambda_1^{(1)}}{2T}\Delta\rho(r) \quad , \tag{101}$$

where the λ-parameters are related to the coefficients of the pion-nucleon scattering amplitude of Eq. (71) by

$$\bar{\lambda}_0^{(1)} = \frac{4\pi p_1 b_0}{k^2} \quad , \tag{102}$$

$$\bar{\lambda}_1^{(1)} = \frac{8\pi p_1 b_1}{k^2} \quad , \tag{103}$$

$$\lambda_0^{(1)} = \frac{4\pi}{p_1} c_0 \quad , \text{ and} \tag{104}$$

$$\lambda_1^{(1)} = \frac{8\pi}{p_1} c_1 \quad . \tag{105}$$

The barred quantities refer to s waves and the unbarred to p waves. The quantities p_1 and p_2 are defined in Eq. 70. As we have indicated, near resonance we expect to have to calculate the amplitudes b and c with a complex energy shift. In second order we find

$$\Delta\xi_0 = \lambda_0^{(2)} \frac{\rho^2(r)}{\rho_0} + \lambda_3^{(2)} \frac{\Delta\rho^2(r)}{\rho_0} - \frac{1}{2T-1} \lambda_2^{(2)} \frac{\Delta\rho^2(r)}{\rho_0} \quad ,$$

$$\Delta\xi_1 = \frac{\lambda_1^{(2)}}{2T} \frac{\rho\Delta\rho}{\rho_0} + \frac{\lambda_2^{(2)}}{2T(2T-1)} \frac{\Delta\rho^2}{\rho_0} \quad , \text{ and} \tag{106}$$

$$\Delta\xi_2 = \frac{\lambda_2^{(2)}}{T(2T-1)} \frac{\Delta\rho^2}{\rho_0} + \frac{\lambda_4^{(2)}}{T^2} \frac{\Delta\rho^2}{\rho_0} \quad ,$$

where the $\lambda^{(2)}$ may be calculated from the cluster expansion of Lecture I, as will be discussed further in Lecture III. Several important results are that $\lambda^{(2)}$ are expected to be strongly energy dependent and weakly dependent on N, Z, and A in the region of the (3,3) resonance. When Coulomb mixing of the nuclear wave functions is taken into account, the quantity $\Delta\rho(r)$ should be taken to be the valence neutron density[49] instead of $\rho_n - \rho_p$.

Experimental results for elastic, single-, and double-charge exchange are being accumulated now very rapidly at the meson factories. I shall describe next our preliminary attempts to understand these results in terms of the theory just described.

The first low-energy single-charge-exchange scattering data have just been taken at LAMPF.[54] The angular distribution is shown in Fig. 13. The parameters of Stricker, McManus, and Carr have been used

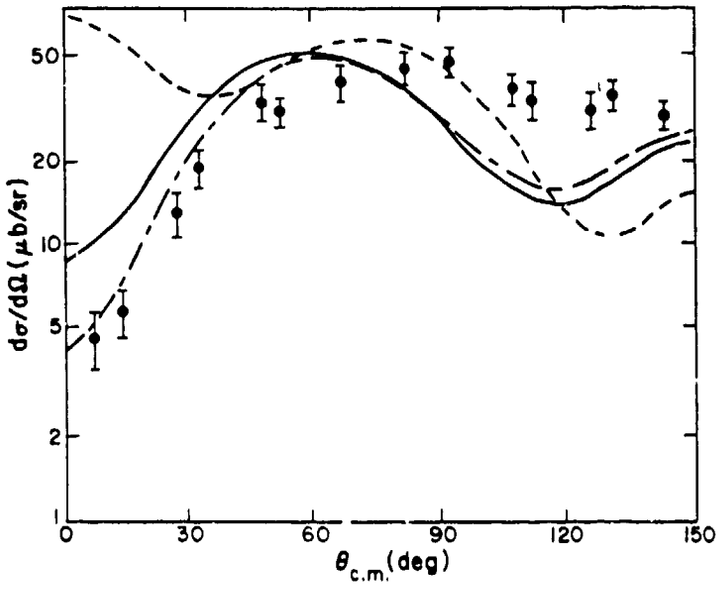

Fig. 13. Angular distribution for pion single-charge exchange to the isobaric analog state of ^{15}N at 48 MeV. The figure is from Ref. 54. The short-dashed curve is calculated without second-order terms. The solid curve includes the isovector Lorentz-Lorenz term and the long-dashed curve includes a small phenomenological adjustment of the second-order isovector term.

for the isoscalar potential. Without any isospin-dependent second-order terms we obtain the short-dashed curve. The discrepancy in the forward direction is striking. Including the isovector second-order $U^{(2)}$ arising from the LLEE term gives the solid curve, which now lies much closer to the data. The physics of this improvement is interesting. At low energy there is a strong tendency for the repulsive s-wave and attractive p-wave terms in the pion-nucleon interaction to cancel in charge-exchange scattering. This gives rise to a dip in the forward direction of the free pion-nucleon amplitude. For pion-nucleus scattering, the interference is strongly modified by multiple scattering. It appears to be a coincidence that the correlation effects again weaken the p waves (see discussion of low-energy elastic scattering in this lecture) sufficiently to restore a large part of the interference observed in free pion-nucleon scattering. With a minor adjustment of the isovector second-order term one could come even closer to the data. The necessary adjustments in the isospin dependence may of course be calculated microscopically from the theory presented in Lecture I.

Let me now move to a discussion of the combined theory of elastic and charge-exchange scattering in the resonance region. A large body of data is beginning to be acquired at these energies, which makes the confrontation of theory and experiment particularly exciting. I will show next some of our attempts to fit the

experimental data with the theory just described, and in Lecture III I will discuss the extent to which the theory and experiment are giving a consistent picture. The results[55] that I will show are preliminary and may change quantitatively as the analysis procedure is made more internally consistent.

The first step in the analysis was designed to determine a single energy shift which would describe elastic scattering for N = Z nuclei throughout the resonance region. Fitting elastic-scattering data for the nuclei ^{16}O, ^{28}Si, and ^{40}Ca we determined that

$$\Delta E = 28.7 + 15i \text{ MeV} \tag{107}$$

would do a reasonably good job of fitting the depths and positions of the first minima for $\pi^{\pm}$ scattering at 165 and 180 MeV. The fits were somewhat better at 180 MeV, and I show in Fig. 14 the result for π^+ scattering on ^{40}Ca at this energy compared to experiment.[56]

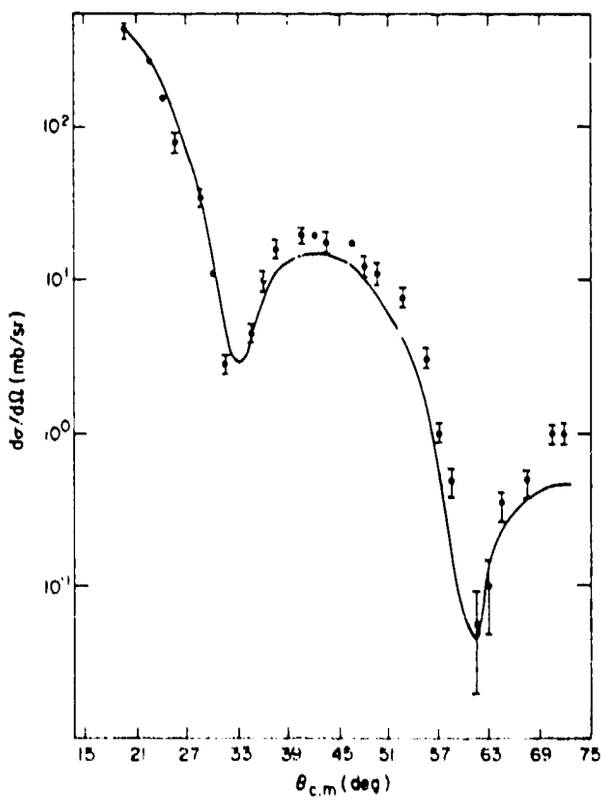

Fig. 14. π^+ elastic scattering from ^{40}Ca at 180 MeV. The theory contains only lowest order terms with an energy shift of $\Delta E = 28.7 + 15i$ MeV.

Using the value of the energy shift in Eq. (107) we next varied the parameters $\lambda_0^{(2)}$ and $\lambda_1^{(2)}$ to obtain a fit to the $\sigma(0^\circ)$ cross section for single-charge exchange at 164 MeV.[57] Without second-order terms, the theory underestimates the data by as much as a factor of two.[53] The parameters of the best fit are

$$\lambda_0^{(2)} = (0.03 - 2.151)\ \text{fm}^3 \quad \text{and} \tag{108}$$

$$\lambda_1^{(2)} = (1.99 + 9.781)\ \text{fm}^3 \quad , \tag{109}$$

and the results are shown in Fig. 15. Note that both the magnitude and the N, Z, and A dependence are very well reproduced. In order to fit the magnitude a rather large isovector coefficient $\lambda_1^{(2)}$ is required.

We next determined $\lambda_2^{(2)}$, the coefficient of the second-order isotensor potential, using the 5° measurements of double-charge exchange at 164 MeV.[58] The results of the fit are shown in Fig. 16. Again we see a generally acceptable reproduction of the data. The best-fit parameter $\lambda_2^{(2)}$ is

$$\lambda_2^{(2)} = (0.08 + 7.041)\ \text{fm}^3 \quad . \tag{110}$$

The value $\lambda_4^{(2)}$ which we used was taken to be

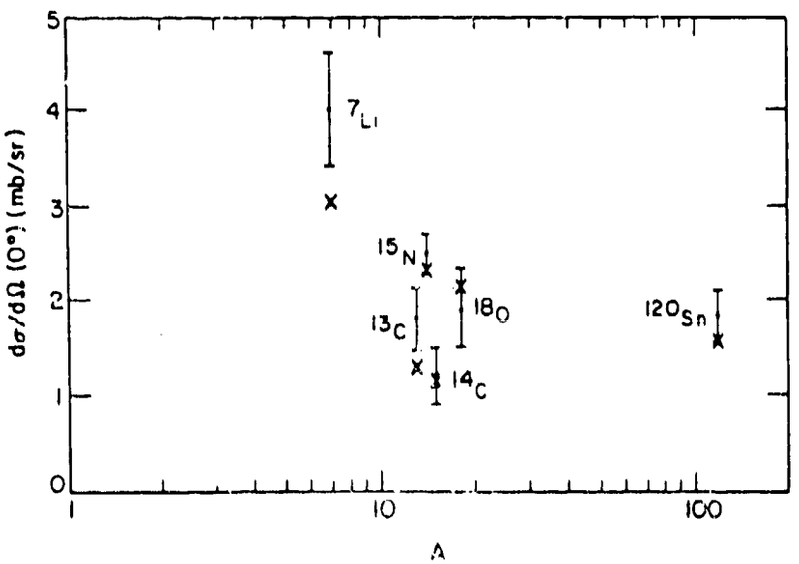

Fig. 15. Zero-degree cross section for SCX at 165 MeV vs A. The crosses are the results of the calculation described in the text.

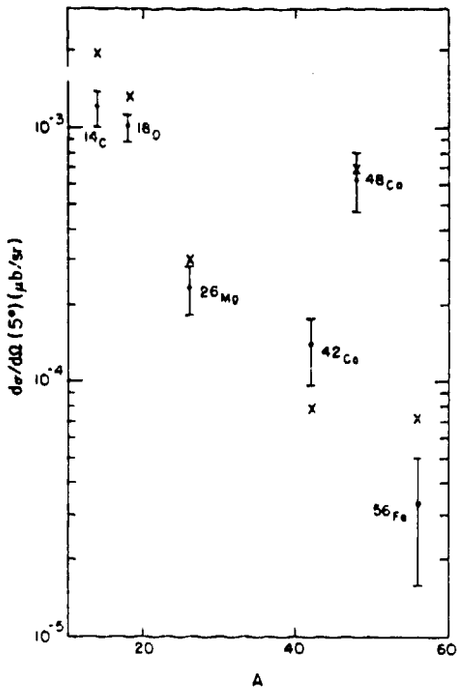

Fig. 16. Five-degree cross section for DCX at 165 MeV vs A. The crosses are the results of the calculation described in the text.

$$\lambda_4^{(2)} = (1.5 + 2i)\ \text{fm}^3 \quad ; \tag{111}$$

this quantity is a theoretically determined number, the origin of which will be discussed in Lecture III. A large value of $\lambda_2^{(2)}$ is required to give the correct scale to the cross sections.

The optical potential is now completely determined empirically. However, there exist angular distributions for double-charge exchange which have been difficult to understand theoretically. The most puzzling is $^{18}O(\pi^+,\pi^-)^{18}Ne$ (Ref. 59), whose first minimum lies at 22°, in contrast to the predictions of most theories, which give this minimum to lie at 30-35°. Using the set of empirically determined parameters, we find the angular distribution shown in Fig. 17. We see that the minimum occurs close to 22° in accordance with the data. The angular distribution for ^{26}Mg has been calculated and also looks quite satisfactory. For ^{14}C the minimum occurs where the minimum of the data appears, but the theory overshoots the second maximum by a factor of four.

What is one to make of these results? At the present time it is hard to draw quantitative conclusions because (1) some of the data are preliminary, (2) the elastic-scattering data at 164 MeV are not reproduced as well as they could be by our energy shift, and (3) the

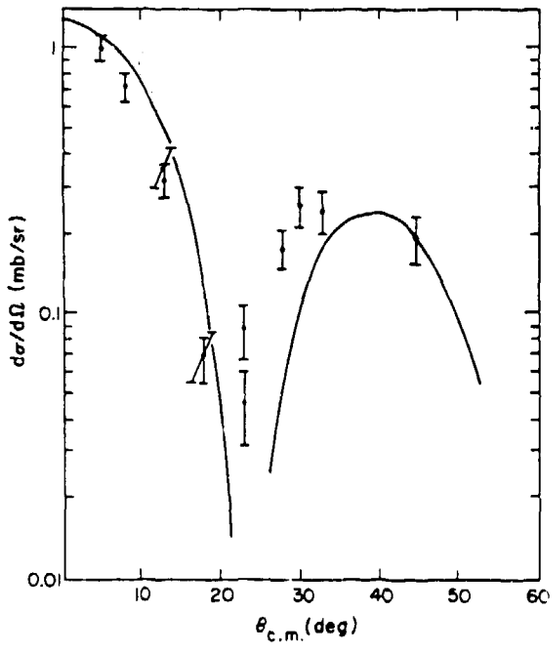

Fig. 17. Angular distribution for $^{18}O(\pi^+,\pi^-)^{18}Ne$ at 165 MeV.

theoretical value of $\lambda_4^{(2)}$ will change as we refine the calculation. I do not expect qualitative changes in the parameters, however, and in the next lecture I will make a comparison to the theory with this in mind. The fact that the trends of the data are so well reproduced by the theory is, I believe, a strong indication that our basic assumptions of isospin invariance and scaling of U with density are valid.

A topic of interest for resonance-energy scattering is application of the eikonal method. It turns out that relatively simple analytic expressions for cross sections and their relationship to the optical potential can be obtained by using this method. This approach has been developed in Refs. 60 and 53. One of the results established there is that the analytic expressions are surprisingly accurate. I do not have time to go into detail, but I would like to end this lecture by pointing out several results which are easily derived using this representation.

One result is that the single- and double-charge-exchange cross sections at zero degrees should be very sensitive to the valence neutron densities. It is shown in Ref. 53 that in the absence of $U^{(2)}$ the sensitivity of the cross sections to N, Z, and A occurs principally as

$$\sigma_{SCX}(0^\circ) \sim \frac{\bar{R}^2}{T}\left(\frac{\Delta\rho(\bar{R})}{\rho(\bar{R})}\right)^2 \quad \text{and} \tag{112}$$

$$\sigma_{DCX}(0^\circ) \sim \bar{R}^2 \left(\frac{2T-1}{T^3}\right) \left(\frac{\Delta\rho(\bar{R})}{\rho(\bar{R})}\right)^4 \quad , \tag{113}$$

where $\bar{R}$ is numerically equal to the impact parameter at which the magnitude of the pion wave function is attenuated by a factor of 1/2 as the pion passes through the nucleus. In practice this occurs at approximately the 10% density point for resonance-energy pions, i.e., where

$$\frac{\rho(\bar{R})}{\rho(0)} \approx 0.1 \quad . \tag{114}$$

The trends of the experimental relative cross sections for SCX and DCX (except ^{48}Ca; see discussion in Lecture III) closely follow Eqs. (112) and (113) with the simple "scaling" densities,[53]

$$\rho_n = \frac{N}{A}\rho \quad \text{and} \tag{115}$$

$$\rho_p = \frac{Z}{A}\rho \quad . \tag{116}$$

The gross features of the cross sections are thus of a geometrical character. However, the fluctuations of the data around the scaling model are significant and depend sensitively on the details of the nuclear wave functions[49] in the way prescribed in Eqs. (112) and (113). One concludes from this that fits to the data such as those in Figs. 15 and 16 could not be obtained unless a reasonably good description of nuclear wave functions was used. We have used throughout our analysis the densities of Ref. 20(a). The effect of the second-order potential is mostly a renormalization of the theory in these figures in a way that is uniform throughout the periodic table.[51]

To summarize, we have relied on the expectation that the nuclear structure is much better known than the reaction theory at the present time to learn something about the latter aspect of the theory. We hope that in the not-too-distant future we will be able to turn the question around to use the newly obtained knowledge of the reaction theory to learn new details of nuclear structure.

III. Evaluation of Higher Order Optical Potential

In Lecture I, I derived a perturbation expansion for the optical potential, U. One of the main worries about such an expansion is that the higher order terms will be found to be large and that the series will not converge. If the higher order terms are so large, we would need in addition to the expansion for U a nontrivial principle for

deciding the order in which to evaluate the expansion. In this lecture I will discuss several of the summation procedures which have been utilized in the literature.

The most straightforward is the "hole-line expansion,"[24] which is in spirit much the same as the spectator expansion[52] discussed in Lecture II. The idea is simply to collect together all terms having one hole line as the leading term in the optical potential. As I have discussed, this sum would give the free pion-nucleon scattering amplitude. The leading correction to this would be the sum of all terms with <u>two</u> hole lines, etc. The rationale for this expansion is that successively higher order corrections involve successively higher powers of the density, and one therefore relies on the hope that the nucleus is of sufficiently low density that the expansion will converge rapidly.

In the event that the second-order correction is large, a more powerful method of summing Eq. (52) would be required. One such method was proposed and studied in Refs. 38 and 61 in a relatively simple potential model. In this case we attempt to evaluate all corrections in terms of "dressed pion propagators," i.e., all internal pion lines in Eq. (52) interact with the medium through the optical potential. The series for U is much more compactly summed, and one must be careful to avoid double counting. Because U is then defined in terms of itself, the problem becomes one of a self-consistent nature. I will come back to this idea later in the lecture.

There may, of course, be other ideas which will prove useful for summing Eq. (52) to obtain the optical potential. As we learn more about the physics we will be better able to distinguish among the various possibilities. We shall turn now to the evaluation of second-order terms in the hole-line expansion.

The second-order terms contributing to B_η in Eq. (50) have the structure shown in Fig. 18; i.e., there is a direct term, Fig. 18(a), and an exchange term, Fig. 18(b). If we let $D(\underline{r}_1,\underline{r}_2)$ denote the value of the diagram to be averaged over the nuclear wave function, then these terms contribute to the optical potential as

$$\text{Fig. 18(a)} = \int d^3r_1 \int d^3r_2 \sum_A \langle\psi_A|\underline{r}_1\rangle \langle\underline{r}_1|\psi_A\rangle \sum_B \langle\psi_B|\underline{r}_2\rangle \langle\underline{r}_2|\psi_B\rangle D(\underline{r}_1,\underline{r}_2) \tag{117}$$

$$\text{Fig. 18(b)} = -\int d^3r_1 \int d^3r_2 \sum_{A,B} \langle\psi_A|\underline{r}_1\rangle \langle\underline{r}_1|\psi_B\rangle \langle\psi_B|\underline{r}_2\rangle \langle\underline{r}_2|\psi_A\rangle D(\underline{r}_1,\underline{r}_2) \ . \tag{118}$$

I have indicated for simplicity only the nucleon coordinate labels in Eqs. (117) and (118). In order to treat charge exchange, the isospin must also be isolated and treated explicitly.

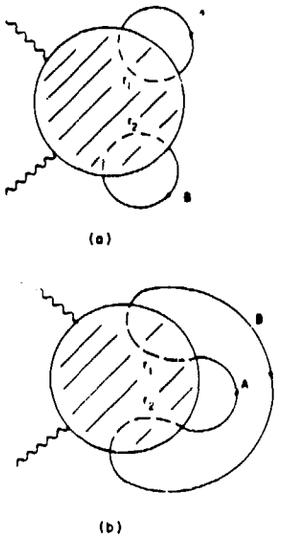

Fig. 18. Classification of terms contributing to Eq. (50) into direct (a) and exchange (b) pieces.

The expressions for Fig. 18 may be written in terms of the density matrix,

$$\rho(\underline{r}_1,\underline{r}_2) = \sum_A \langle \underline{r}_2|\psi_A\rangle \langle\psi_A|\underline{r}_1\rangle \quad . \tag{119}$$

Thus, Eq. (117) is expressed in terms of the product

$$n(r_1,r_2) \equiv \rho(r_1,r_1)\rho(r_2,r_2) \quad , \tag{120}$$

and Eq. (118) in terms of

$$n(r_1,r_2) = \rho(\underline{r}_1,\underline{r}_2)\ \rho(\underline{r}_2,\underline{r}_1) \quad . \tag{121}$$

Simplifications become possible when the density matrices are expanded around their nuclear matter values.[20(a)] The local density approximation (LDA) specifies

$$\rho(\underline{r}_1,\underline{r}_2) \equiv \rho(R)S_F(k_F r) \quad , \tag{122}$$

where

$$\underset{\sim}{R} = (\underset{\sim}{r}_1 + \underset{\sim}{r}_2)/2 \quad \text{and} \tag{123}$$

$$\underset{\sim}{r} = \underset{\sim}{r}_1 - \underset{\sim}{r}_2 \quad . \tag{124}$$

The density matrix in Eq. (122) is evaluated in terms of the nuclear matter Slater function,

$$S_F(x) = \frac{3}{x^3} (\sin x - x \cos x) \quad , \tag{125}$$

and local Fermi momentum $k_F(R)$,

$$k_F^3 = 3\pi^2 \rho(R) \quad . \tag{126}$$

If we apply the LDA separately to neutrons and protons, we are able to write an expansion of U in terms of the quantities $\rho(R) = \rho_n(R) + \rho_p(R)$ and $\Delta\rho(R) = \rho_n(R) - \rho_p(R)$.

Let me now make several technical comments about refinements for the LDA which have been used for the practical evaluation of U in this theory. The LDA is designed to apply exactly for an infinite system, whereas for pion scattering near resonance the most important densities correspond to the nuclear surface region. We therefore need to apply a correction. We make the correction assuming that the density in the surface behaves as

$$\rho(r_1) \approx \rho(R) e^{-(r_1 - R)/a} \quad . \tag{127}$$

If we take the diffuseness $\underline{a}$ to depend on R as

$$a(R) = -\rho(R)/\rho'(R) \quad , \tag{128}$$

then the exponential expression in Eq. (127) may be expected to represent $\rho(r)$ locally around any R.

The expression Eq. (127) may be simplified. For scattering in the resonance region we may think of the pion as traveling along a trajectory which is a straight line of impact parameter b parallel to the Z axis. The important interactions occur where these trajectories just graze the nuclear surface; pions moving along trajectories of smaller impact parameter are readily absorbed out of the elastic channel. Because of this, the most important interactions occur where $\underset{\sim}{R}$ is large and $\underset{\sim}{r}$ is small, so

$$r_1 = |\underset{\sim}{R} + \frac{\underset{\sim}{r}}{2}| \approx \underset{\sim}{R} + \frac{r^2}{8R} + \frac{\hat{R} \cdot \underset{\sim}{r}}{2} + \ldots . \qquad (129)$$

We may drop the term $\hat{R} \cdot \underset{\sim}{r}/2$ because $\underset{\sim}{R}$ and $\underset{\sim}{r}$ are nearly perpendicular. Inserting Eq. (129) into Eq. (127), we find for the direct term in Fig. 18

$$n(r_1, r_2) = \rho^2(R) e^{-r^2/4Ra} \quad . \qquad (130)$$

A similar approximation is plausible for the exchange term, and we take

$$n(\underset{\sim}{r}_1, \underset{\sim}{r}_2) = \rho^2(R) S_F^2(k_F r) e^{-r^2/4Ra} \quad . \qquad (131)$$

If one now evaluates the terms contributing to Fig. 18 using the diagram rules of Lecture I, employing the spectator expansion of Eqs. (94) and (96), and using these approximations for the density matrices, one finds that $U^{(2)}$ can be cast into the following form,

$$\hat{U}^{(2)} = U_0^{(2)} + U_1^{(2)} \underset{\sim}{\ell} \cdot \underset{\sim}{T} + U_2^{(2)} (\underset{\sim}{\ell} \cdot \underset{\sim}{T})^2 \ , \qquad (132)$$

where

$$U_i^{(2)} = - \frac{v(k)v(k')}{v^2(k_0)} k_0^2 \hat{e}'_k \cdot \hat{e}_k \int d^3R \ e^{-i\underset{\sim}{R} \cdot (\underset{\sim}{k}' - \underset{\sim}{k})} \Delta\xi_i(R) \qquad (133)$$

and where $\Delta\xi_i(R)$ is given in Eq. (106). We have assumed that the interaction amplitudes out of which the diagrams are built act in relative pion-nucleon p waves; this then leads to the characteristic p-wave $\hat{e}'_k \cdot \hat{e}_k$ form ($\hat{e}'_k$ is a unit vector in the direction of k'). If s waves are important, then $U_i^{(2)}$ would contain other partial-wave contributions with the corresponding ξ_i of the same form as Eq. (106). Note that the coefficients $\lambda_i^{(2)}$ in Eq. (106) are integrals over the relative coordinate $\underset{\sim}{r} = \underset{\sim}{r}_1 - \underset{\sim}{r}_2$; the evaluation of the $\lambda_i^{(2)}$ corresponding to a given diagram is straightforward but nontrivial. Further details may be found in Ref. 50.

I want to consider next the results of the evaluation of $\lambda_i^{(2)}$ corresponding to the sequential scattering terms. A few of the sequential terms were already mentioned in connection with Fig. 6, and I have collected the relevant terms in Fig. 19. Figure 19(a) and (b) are the direct and exchange matrix elements of the sequential scattering processes. Figure 19(c) is the once-iterated lowest order optical potential which must be subtracted from the sum of Fig. 19(a) and (b)

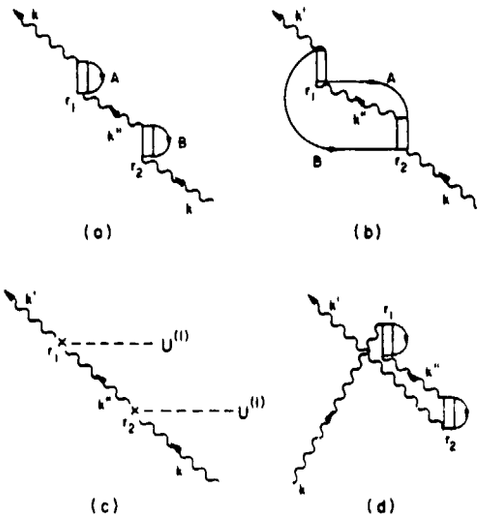

Fig. 19. Two-nucleon processes contributing to the pion-nucleus optical potential. These terms are second order in the pion-nucleon scattering amplitude and are referred to as sequential scattering processes.

as indicated in Eq. (93). Figure 19(d) is the crossed process corresponding to Fig. 19(a). It can be easily verified that Fig. 19(a), (b), and (c) are automatically crossing symmetric if the pion-nucleon amplitude is crossing symmetric; the sequential processes are therefore examples of terms for which it would be wrong to add an explicit crossed term in Eq. (53).

It is interesting to note that the iteration of the lowest order optical potential [Fig. 19(c)] needed in evaluating the spectator expansion in Eq. (93) picks up contributions only from intermediate analog states. This follows from the relationship

$$\underline{\phi} \cdot \underline{T}_N \, |\pi^+ gs\rangle = 2\sqrt{T} \, |\pi^0 A^{(1)}\rangle \quad . \tag{134}$$

One consequence is that the contribution to $\Delta\zeta^{(2)}$ arising from the subtraction of the lowest order optical potential has the form

$$\Delta\zeta^{(2)}(-\langle U^{(1)} G_0 U^{(1)}\rangle) = \frac{\lambda_4^{(2)}}{T^2} \frac{\Delta\rho^2(r)}{\rho_0} \quad . \tag{135}$$

On the other hand, Fig. 19(a) and (b) allow for the sequential scattering to $|A^{(2)}\rangle$ through <u>all</u> possible intermediate states. One does not see explicitly the <u>sum</u> over all states because the assumption of fixed nucleons is equivalent to performing this sum in a closure

approximation.[6] To convert these amplitudes for elastic scattering into a contribution to the isotensor potential, we use Eq. (96),

$$U^{(2)} = \frac{1}{T(2T-1)}\left[U^{(+)} + U^{(-)} - 2U^{(0)}\right] , \tag{136}$$

and obtain

$$\Delta\zeta^{(2)}(\text{closure}) = \frac{\lambda_2^{(2)}}{T(2T-1)}\,\frac{\Delta\rho^2(R)}{\rho_0} . \tag{137}$$

Note that Eqs. (135) and (137) have different dependence on T. One finds that the diagram in Fig. 19(c) is the only one that contributes to $\lambda_4^{(2)}$, whereas all other terms in the expansion for $U^{(2)}$ contribute to $\lambda_2^{(2)}$ in Eq. (137). We shall see that this T dependence of the isotensor potential is important in understanding the double-charge-exchange data.

The optical potential as given in Eq. (106) will be most useful if the strongest dependence on N, Z, and A is contained in the explicit factors of T, ρ, and $\Delta\rho$. If this is the case, then the parameters $\lambda_i^{(2)}$ can be calculated once and for all at a given energy, and they would characterize scattering throughout the periodic table. We can see the extent to which this is true for the sequential scattering by referring to Fig. 20, which shows the $\lambda^{(2)}$ for these terms. The calculation was performed as just described, utilizing a short-ranged correlation function which cuts off sharply at 0.5 fm. The contribution of the ρ-meson exchange between the nucleons was not considered.

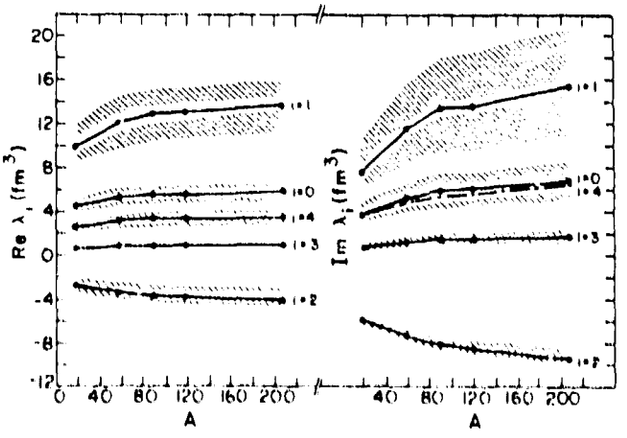

Fig. 20. Calculated parameters characterizing the second-order sequential contributions to the optical potential at T_π = 180 MeV as a function of nuclear mass number A. The solid dots result from evaluating U(R) at R = $\bar{R}$ (see discussion of Eqs. (112) and (113). The hatch marks show the change in $\lambda_i^{(2)}$ as $\bar{R}$ is varied by ±0.5 fm.

We note that the $\lambda_i^{(2)}$ shown in Fig. 20 are independent of N-Z to a very good approximation. The coefficients have a weak dependence on A and R, especially apparent for $\mathrm{Im}\lambda_2^{(2)}$ and $\mathrm{Im}\lambda_1^{(2)}$. Calculating the $\lambda^{(2)}$ as a function of energy we find, as expected, a very strong dependence on the pion energy.

In our fit to elastic, single-, and double-charge-exchange data presented in Lecture II, we took the parameters $\lambda_i^{(2)}$ to be constant as a function of N, Z, and A and also independent of R. Because of the residual dependence of $\lambda_i^{(2)}$ on R and A, the empirical parameters represent averages $\langle\lambda_i^{(2)}\rangle$ over the periodic table where the data exist. We would expect some weak, systematic, A-dependent discrepancies in the fits to the data arising from variations of $\lambda_i^{(2)}$ around $\langle\lambda_i^{(2)}\rangle$. This discrepancy is not, however, prominent in the fit to SCX due to the fact that a large portion of the scattering occurs through terms linear in the nuclear densities. For the case of DCX, data exist only for relatively light nuclei where the percentage variation of the $\lambda_i^{(2)}$ with A as seen in Fig. 20 is still small.

The empirical determination of $\lambda_i^{(2)}$ is very interesting because it bears directly on our understanding of the many-body problem of strongly interacting particles. We have discussed in detail a theory of these quantities, and a comparison of theory to experiment will indicate the extent to which our ideas are valid.

In order to compare the values of the coefficients in Eqs. (108), (109), and (110) to the predictions for the sequential terms, we must choose an energy at which to evaluate the latter. Due to the possibility of energy shifts, it is not clear, without further theoretical study, what this energy should be. If we choose the incident pion energy, 164 MeV, then we find

$$\lambda_0^{(2)} = 7.25 + 0.97i \text{ fm}^3 \tag{138}$$

$$\lambda_1^{(2)} = 15.4 + 1.40i \text{ fm}^3 \tag{139}$$

$$\lambda_2^{(2)} = -6.0 - 4.6i \text{ fm}^3 \quad . \tag{140}$$

In the case of the isovector optical potential, I believe it is significant that both the theory and the calculation give large values for $\lambda_1^{(2)}$. The piece of the theory which makes $\lambda_1^{(2)}$ large is the Pauli term, Fig. 20(b); i.e., the effect of short-ranged correlations is small. The theoretical value is 50% larger than the experimental result and differs in phase by 73°. A decrease in the magnitude of $\lambda_1^{(2)}$ and a rotation of phase in the desired direction would occur if one were to use the medium-modified pion-nucleon scattering amplitude $\bar{f}$

discussed at the end of Lecture III in evaluating this term, instead of the free pion-nucleon scattering amplitude.

In the case of the isoscalar potential $\lambda_0^{(2)}$ we again find that the Pauli term dominates. Now, however, the theoretical and empirical values differ greatly in both phase and magnitude. This lack of agreement is not surprising in view of the expectation that the Pauli terms will be balanced and perhaps dominated by collisional broadening effects, which we have not yet considered (see discussion later in this section).

The isotensor potential coefficient $\lambda_2^{(2)}$ is of the same magnitude in the theory and experiment but differs in phase by 140°. The origin of the empirical value is something of a mystery for the microscopic theory, and we return to a more detailed discussion of this term a bit later in the lecture.

We are able to make a somewhat stronger statement about our understanding of the dependence of the isotensor potential on N-Z. It had been something of a puzzle in the empirical study of the T dependence of $d\sigma/d\Omega$ (5°) for DCX why ^{48}Ca (which has T = 4) has a cross section so much smaller than the one predicted by the semiclassical result in Eq. (113). We can now understand this as a manifestation of the fact that the iteration of $U^{(1)}$ yields a cross section with the wrong T dependence. Using our knowledge of the T dependence of the isotensor potential corresponding to the iterated $U^{(1)}$ [Eq. (135)] and the closure result [Eq. (137)], we find to lowest order in $U^{(2)}$

$$\frac{d\sigma}{d\Omega}\ (\text{closure}) = C\left(\frac{2T-1}{T}\right)^2 \frac{d\sigma}{d\Omega}\ [\text{no } U^{(2)}] \quad , \tag{141}$$

where the constant C can be determined from the details of the dynamical model. Taking Eq. (113) for the right-hand side in Eq. (141) we obtain

$$\frac{d\sigma}{d\Omega}\ (0^\circ) = \frac{C'\bar{R}^2}{T(2T-1)}\left[\frac{\Delta\rho(\bar{R})}{\rho(\bar{R})}\right]^4 \quad . \tag{142}$$

We compare in Table I the experimental forward double-charge-exchange cross sections at 165 MeV to the theory using the scaling densities of Eqs. (115) and (116). The experimental numbers are from Refs. 62 and 63. Note that the theory is substantially larger than the experiment for ^{48}Ca without $U^{(2)}$, as emphasized in Ref. 63. When the calculation is repeated using Eq. (142), then the agreement is much improved.

The details of the theory in Table I will change when more realistic densities are used. There is some reason to believe that the value of the cross section for ^{42}Ca would be particularly sensitive to

these improvements through core polarization.[64] Our main point is, however, that it is important to consider nonanalog intermediate states in double-charge exchange, especially for nuclei with large T.

Table I. T dependence of (π^+,π^-) to isobaric analog states at T_π = 165 MeV. The theory is normalized to ^{18}O.

Target	T	Exp. (μb/sr)	Theory	Comment
^{18}O	1	1 ± 0.1	1	
^{26}Mg	1	0.3 ± 0.1	0.29	
^{42}Ca	1	0.14 ± 0.04	0.06	
^{48}Ca	4	0.29 ± 0.13	1.07	no $U^{(2)}$
^{48}Ca	4	0.29 ± 0.13	0.27	with $U^{(2)}$

In the future we will see more effort devoted to the evaluation of the other second-order terms of U, some of which are redrawn in Fig. 21. Figure 21(a) refers to multiple reflections between two nucleons, which we shall see leads to large collision broadening. Figure 21(b) is a term in which the Δ_{33} interacts with the nucleus, and Fig. 21(c) and (d) correspond to the pion interacting with Δ_{33} components in the initial or final nuclear ground state. There may be other more exotic terms; for example, excitation of T = 2 dibaryon states[65] illustrated in Fig. 22.

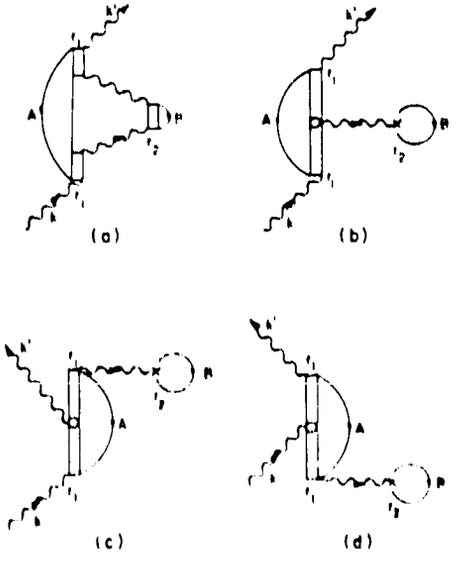

Fig. 21. Additional two-nucleon processes contributing to the pion-nucleus optical potential. (a) is third order in the pion-nucleon scattering amplitude and is referred to as a multiple reflection, whereas (b)-(d) involve various isobar-medium effects. Each process has a corresponding exchange and crossed piece.

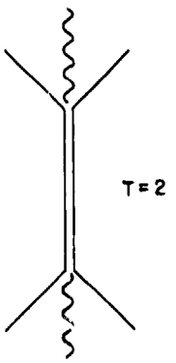

Fig. 22. A speculative term which would contribute to double-charge exchange.

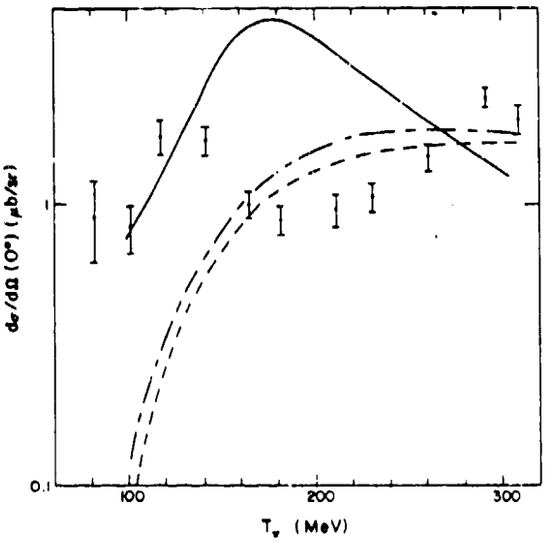

Fig. 23. Five-degree cross section for $^{18}O(\pi^+,\pi^-)^{18}Ne$ as a function of energy The long/short-dashed curve is the sequential process. The short-dashed curve is the sequential plus Fig. 21(c) and (d). The solid curve is sequential plus Fig. 21(b).

The "double delta" terms in Fig. 21(c) and (d) have been of a great deal of interest lately[66] in understanding the connection between analog and nonanalog double-charge exchange. It has been speculated, in particular, that an interference between these terms and the sequential scattering terms might be responsible both for moving the minimum in the $^{18}O(\pi^+,\pi^-)^{18}Ne$ differential cross section to 22° (in the manner discussed in Lecture II) and for the characteristic energy dependence of the excitation function,[67] shown in Fig. 23 for $^{18}O(\pi^+,\pi^-)^{18}Ne$. We have calculated these terms and in addition, the Δ_{33} interacting with the nucleus, Fig. 21(b). Figure 21(b) is large because when one of the Δ_{33} is on resonance, so is the other. Figure 21(b) is, in particular, larger than the terms in Fig. 21(c) and (d), which contain at most one resonant Δ_{33}.

The results of our calculation are based on the assumption that the two neutrons in ^{18}O are in the $(d_{5/2})^2$ configuration. We allow the Δ_{33} to interact with the nucleus through both π- and ρ-meson exchange. The contribution of Fig. 21(c) and (d) is dominated by the tensor component of this interaction, and these terms are therefore reduced when the ρ meson is included. The term in Fig. 21(b) is determined by a combination of the tensor and spin-spin interaction in such a way that, for strong ρ coupling [see Eq. (19)] and short-ranged form factors [$\Lambda_{\rho\Delta\Delta}$ = 1.2 GeV/c--see Eq. (35)], the contribution of

this term is dominated by the ρ meson. Its precise value is very sensitive to $f_{\rho\Delta\Delta}$ and $\Lambda_{\rho\Delta\Delta}$.

The results[68] are shown in Fig. 23. For purposes of comparison we show the iterated $U^{(1)}$ (long-short dashes). It has the right order of magnitude, but undershoots the data at low energy and overshoots it above resonance. When the contribution of Fig. 21(b) is added with strong ρ coupling and $\Lambda_{\rho\Delta\Delta} = 1.2$ GeV/c, we get the solid curve. The agreement with experiment is vastly improved at lower energies, but the theory overshoots the cross section in the vicinity of the resonance by more than a factor of four. We find some tendency for the minimum of the angular distribution at 164 MeV to move in the proper direction (it comes in to 28°). Because of the strong sensitivity to $f_{\rho\Delta\Delta}$ and $\Lambda_{\rho\Delta\Delta}$, the results of the calculation of Fig. 23(b) are very model dependent. This is true to a much lesser extent for the results of Fig. 21(c) and (d). These terms contribute through a higher order tensor in $U^{(2)}$, which we have added to Eq. (133). The short-dashed curve in Fig. 23 is the sum of the sequential plus Fig. 21(c) and (d). We turned the ρ-meson coupling off to enhance the contribution of Fig. 21(c) and (d), and it is seen that even then the result is essentially negligible.

Thus we have found a large contribution of Fig. 21(b) and a small contribution of Fig. 21(c) and (d). Unfortunately, we are unable to understand the data with the combination of the sequential plus double Δ terms. We have also been unable to find a conventional term which, when added to those we have evaluated, will give the experimental results. The main terms which remain to be evaluated are the multiple reflection and true absorption pieces. Of these two contributions to the isotensor potential, the true absorption will be relatively small because the neutron pairs have $T = 1$, and true absorption occurs dominantly on $T = 0$ pairs.[69] The multiple reflection will be much larger, but its phase is similar to that of the sequential processes and will therefore not reproduce the structure in the data. A term which would have the correct phase is a (broad) resonance such as that shown in Fig. 22 with an energy of several hundred MeV above the Δ_{33}.

Let me now turn to the final topic of these lectures, which comes back to a question raised at the beginning of Lecture III, namely, what to do when higher order terms in U become too large to evaluate perturbatively. A case in point is the multiple reflection term in Fig. 21(a), which has been found to be large in heavy nuclei.[70] The idea proposed in Refs. 38 and 61 is that the pion cloud around the Δ_{33} should be allowed to interact with neighboring nucleons in a self-consistent fashion. This leads to a definition of the self-consistent pion-nucleon scattering amplitude $\bar{t}$ and the medium-modified pion propagator $\bar{G}$, which are then to be used for evaluating all higher order corrections. It was shown in Ref. 61 that the new expansion appears to converge faster than the hole-line expansion in the resonance region, and the reasons for expecting this improved convergence throughout all orders was indicated.

The study reported in Refs. 38 and 61 was made in a static potential model for the case of an infinite medium, but the ideas can be extended to more comprehensive theories such as the field theoretical model which is being developed here.[71] Let me describe briefly the static potential model theory, which was applied to evaluate the isoscalar term in the amplitude $\tilde{f}$.

The equations determining $\tilde{f}$ are shown in Fig. 24. In the actual calculations, $\tilde{f}$ was evaluated by solving an integral equation implied by the sequence in Fig. 24(b). Because the pion self-energy is defined in terms of $\tilde{f}$, the equation is nonlinear. Short-ranged correlations were allowed to act between all successively struck nucleons. The pion-nucleon form factor was assumed to have the form given in Eq. (75) with Λ = 765 MeV/c [see discussion below Eq. (75)]. The self-energy in Fig. 24(c) was fit to a Breit-Wigner function. The terms included were: $\tilde{f}$ plus all other legitimate direct multiple reflections of a dressed pion between two nucleons. By a dressed pion, I mean that the pion propagator was the sequence in Fig. 24(d). From this Breit-Wigner parameterization it was possible to determine W_0 and then to compare it to the phenomenological values of isobar-hole model [see Eq. (75) and Fig. 10]. The results are plotted as the solid lines in Fig. 25. The agreement is not perfect, but one

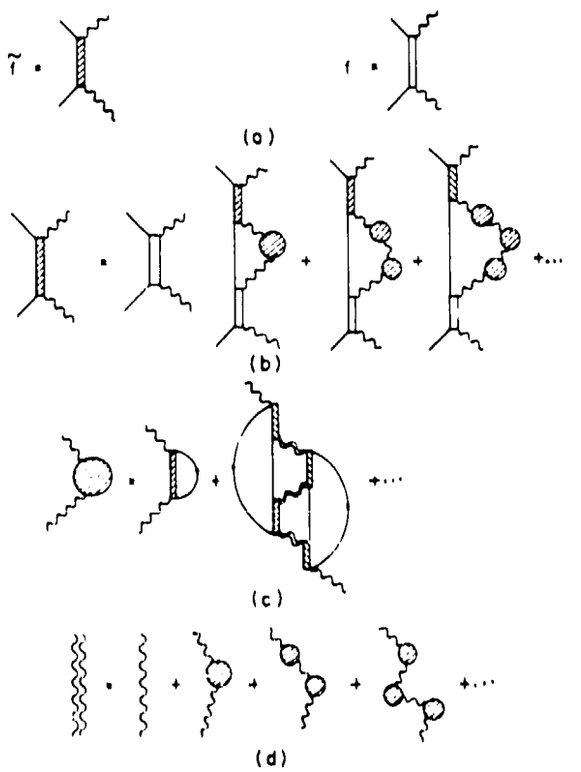

Fig. 24. Coupled equations determining the self-consistent pion-nucleon scattering amplitude $\tilde{f}$ in terms of the free amplitude f.

sees that the magnitude and sign of the empirical isobar-nucleus isoscalar potential is repro uced by this calculation. If this spreading interaction is converted to a second-order isoscalar optical potential, it contributes a large <u>negative</u> value for $\mathrm{Im}\lambda_0^{(2)}$ at 164 MeV, as it corresponds to a broadening of the Δ_{33} resonance. This sign for $\mathrm{Im}\lambda_0^{(2)}$ is the same as the empirical value given in Eq. (108). Consistency between the empirical $\lambda_0^{(2)}$ and the theoretical calculation would thus indicate that the collision-broadening terms dominate over the resonance-narrowing (Pauli) term in Eq. (138).

The main result of this lecture, given in Eqs. (133) and (106), is the parameterization of $U^{(2)}$, appropriate for resonance-energy scattering. We found that this form is justified as a low-density approximation in the static Chew-Wick field theory with $\lambda^{(2)}$ nearly independent of N-Z, weakly dependent on A and R, and strongly dependent on energy. We were able to draw tentative conclusions about the theory based on a partial evaluation of the parameters contributing to $U^{(2)}$. Considerations of enhancing the convergence of the expansion of U lead to the notion of self-consistency. We showed that the qualitative behavior of the isoscalar optical potential is determined by the self-consistent determination of the pion-nucleon scattering amplitude in the medium. We concluded that the large empirical value for the isovector optical potential found in Lecture II could arise from the Pauli correlations calculated in terms of the self-consistent pion-nucleon scattering amplitude. To implement a fully self-consistent calculation of $U^{(2)}$ following the ideas presented in Refs. 38 and 61 would require a somewhat generalized definition of a second-order correction to U. One would hope that the result

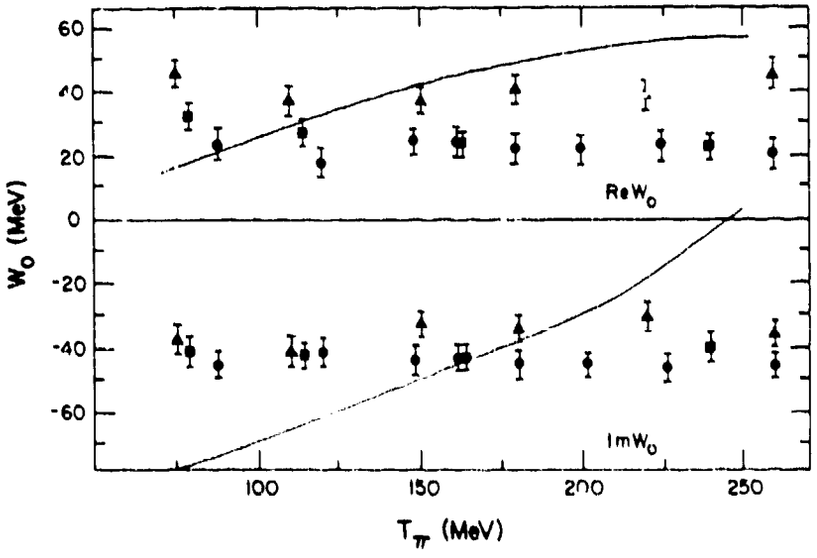

Fig. 25. Comparison of the theoretical spreading potential of Ref. 61 to the phenomenological result of Ref. 4(a). The legend is the same as Fig. 10.

would not differ drastically in form from Eqs. (133) and (106); e.g., that allowing $\lambda_1^{(2)}$ to have a (weak) dependence on $\rho(R)$ would be sufficient.

The isotensor potential is the most poorly understood component of $U^{(2)}$. We found evidence for the necessity of including intermediate nonanalog states in sequential scattering by considering the relative forward cross section of double-charge exchange from ^{48}Ca compared to that for T = 1 nuclei. In trying to understand the absolute magnitude of the DCX cross section, we showed that the Δ_{33} interacting with the nucleus would give a large enhancement to double-charge exchange but that this would not describe the data for energies above 140 MeV. If one adopts the strong ρ coupling to the Δ_{33} and a high mass $\rho\Delta\Delta$ form-factor cutoff, what appears to be needed is a term in $U^{(2)}$ which behaves like a broad resonance with a mass 100-200 MeV above that of the Δ_{33} resonance.

How close have we come to solving the basic problems as put forth in the introduction to these lectures? It is certainly too early to claim to have a completely satisfactory solution. However, I am encouraged by successes we have had in the phenomenological application of the ideas and by hints that the dominant physics of the isoscalar and isovector second-order terms has been identified. We hope to have a more complete determination of the second-order optical potential in the future. Because of the large energy shifts found in the empirical studies, one would like to embed $U^{(2)}$ in a calculation for which the lowest order potential is obtained from first principles. Progress in this direction is being made (see Ref. 42). Some consideration for the extension of the theory of $U^{(2)}$ beyond the static approximation would also be desirable. Once a reasonably well-justified dynamical model of U is obtained, we will be much closer to the long-sought goal of being able to study nuclear structure quantitatively with pions.

References

1. K. M. Watson, Phys. Rev. 89, 575 (1953); and A. Kerman, H. McManus, and R. Thaler, Ann. Phys. (N.Y.) 8, 552 (1959).
2. A. L. Fetter and J. D. Walecka, Quantum Theory of Many-Particle Systems (McGraw-Hill, New York, 1971).
3. R. H. Landau, S. C. Phatak, and F. Tabakin, Ann. Phys. (N.Y.) 78, 299 (1973); M. G. Piepho and G. E. Walker, Phys. Rev. C9, 1352 (1974); E. R. Siciliano and G. E. Walker, Phys. Rev. C13, 257 (1976); and R. H. Landau and A. W. Thomas, Nucl. Phys. A302, 461 (1978).
4. (a) Y. Horikawa, M. Thies, and F. Lenz, Nucl. Phys. A345, 386 (1980); (b) M. Hirata, J.-H. Koch, F. Lenz, and E. J. Moniz, Ann. Phys. (N.Y.) 120, 205 (1979); and (c) M. Hirata, F. Lenz, and K. Yazaki, Ann. Phys. (N.Y.) 108, 116 (1977).

5. M. B. Johnson and D. J. Ernst, Phys. Rev. C20, 1064 (1979).
6. M. B. Johnson and D. J. Ernst, Phys. Rev. C27, 709 (1983).
7. E. Oset, H. Toki, and W. Weise, Phys. Rep. 83, 281 (1982).
8. G. E. Brown and W. Weise, Phys. Rep. 22, 279 (1975).
9. H. Sugawara and F. Von Hippel, Phys. Rev. 172, 1764 (1968).
10. T. DeGrand, R. L. Jaffe, K. Johnson, and J. Kiskis, Phys. Rev. D12, 2060 (1975).
11. G. E. Brown and M. Rho, Phys. Lett. 82B, 177 (1979).
12. S. Théberge, A. W. Thomas, and G. A. Miller, Phys. Rev. D22, 2838 (1980).
13. G. E. Brown, J. W. Durso, and M. B. Johnson, Nucl. Phys. A397, 447 (1983).
14. U.-G. Meissner and J. W. Durso, State University of New York preprint, Stony Brook, New York, 1983.
15. J. W. Durso, A. D. Jackson, and B. J. VerWest, Nucl. Phys. A282, 404 (1977); and M. Dillig and M. Brack, J. Phys. G5, 223 (1979).
16. D. J. Ernst and M. B. Johnson, Phys. Rev. C17, 247 (1978); and Phys. Rev. C22, 651 (1980).
17. J. T. Londergan, K. W. McVoy, and E. J. Moniz, Ann. Phys. (N.Y.) 86, 147 (1974).
18. S. Barshay, G. E. Brown, and M. Rho, Phys. Rev. Lett. 32, 787 (1974).
19. The phase factor in Eq. (39) was not included in the rules stated in Ref. 4, but it is consistent with the application of closure as discussed there.
20. (a) J. W. Negele and D. Vautherin, Phys. Rev. C5, 1472 (1972); and (b) M. Beiner et al., Nucl. Phys. A238, 29 (1975).
21. J. B. Cammarata and M. Banerjee, Phys. Rev. Lett. 31, 610 (1973); and Phys. Rev. C13, 299 (1976).
22. L. Celenza, L. C. Liu, and C. M. Shakin, Phys. Rev. C12, 194 (1975).
23. E. R. Siciliano and R. M. Thaler, Ann. Phys. (N.Y.) 115, 191 (1978).
24. C. B. Dover and R. H. Lemmer, Phys. Rev. C7, 2312 (1973).
25. D. J. Ernst and M. B. Johnson, to be published.
26. D. J. Ernst and R. McCloud, to be published in Phys. Rev. C.
27. M. Ericson and T. E. O. Ericson, Ann. Phys. 36, 323 (1966).
28. K. Stricker, H. McManus, and J. A. Carr, Phys. Rev. C19, 929 (1979); K. Stricker, J. A. Carr, and H. McManus, Phys. Rev. C22, 2043 (1980); and K. Stricker, Ph.D. thesis, Michigan State University, 1979 (unpublished).
29. L. S. Kisslinger, Phys. Rev. 98, 761 (1955); R. Mach, Nucl. Phys. A205, 56 (1973); and M. Thies, Phys. Lett. 63B, 43 (1976).
30. G. E. Brown, B. K. Jennings, and V. Rostokin, Phys. Rep. 50, 227 (1979).
31. N. J. DiGiacomo, A. S. Rosenthal, E. Rost, and D. A. Sparrow, Phys. Lett. B66, 421 (1977).
32. G. Baym and G. E. Brown, Nucl. Phys. A247, 395 (1975).
33. J. Delorme and M. Ericson, Phys. Lett. 60B, 451 (1976).
34. There are other explanations for the weakening of the optical potential at low energy, i.e., through unitarity or, equivalently,

a self-consistent treatment of the optical potential. See Refs. 35 through 37.
35. H. A. Bethe, Phys. Rev. Lett. 30, 105 (1973).
36. S. Barshay, V. Rostokin, and G. Vagradov, Phys. Lett. 43B, 271 (1973).
37. S. Barshay, V. Rostokin, and G. Vagradov, Nucl. Phys. B59, 189 (1973).
38. M. B. Johnson and H. A. Bethe, Nucl. Phys. A305, 418 (1978).
39. B. M. Preedom et al., Phys. Rev. C23, 1134 (1981).
40. R. Amado, F. Lenz, and K. Yazaki, Phys. Rev. C18, 918 (1978).
41. J. W. Negele, Phys. Rev. C1, 1260 (1970).
42. D. J. Ernst and M. B. Johnson, to be published.
43. W. B. Cottingame and D. B. Holtkamp, Phys. Rev. Lett. 45, 1828 (1980).
44. R. S. Bhalerao, L. C. Liu, and C. M. Shakin, Phys. Rev. C21, 2103 (1980).
45. D. J. Ernst, G. A. Miller, and D. L. Weiss, Phys. Rev. C (to be published).
46. G. A. Miller and J. F. Spencer, Ann. Phys. (N.Y.) 100, 562 (1976); M. Koren, Ph.D. thesis, MIT, 1969 (unpublished); and E. Rost and G. W. Edwards, Phys. Lett. 37B, 247 (1971).
47. L. A. Charleton, J. M. Eisenberg, and W. B. Jones, Nucl. Phys. A71, 625 (1971).
48. N. Auerbach and N. Van Giai, Phys. Rev. C24, 782 (1981).
49. N. Auerbach, M. B. Johnson, A. Klein, and E. R. Siciliano, (to be published).
50. M. B. Johnson and E. R. Siciliano, Phys. Rev. C27, 730 (1983).
51. M. B. Johnson and E. R. Siciliano, Phys. Rev. C27, 1647 (1983).
52. E. R. Siciliano and R. M. Thaler, Phys. Rev. C16, 1322 (1977).
53. M. B. Johnson, Phys. Rev. C22, 192 (1980).
54. M. D. Cooper, H. W. Baer, R. Bolton, J. D. Bowman, F. Cverna, N. S. P. King, M. Leitch, J. Alster, A. Doron, A. Erell, M. A. Moinester, E. Blackmore, and E. R. Siciliano (unpublished).
55. R. Gilman, S. Greene, C. Harvey, M. B. Johnson, E. R. Siciliano, and P. Seidl (unpublished).
56. C. L. Morris, K. C. Boyer, C. F. Moore, C. J. Harvey, K. J. Kallianpur, I. B. Moore, P. A. Seidl, S. J. Seestrom-Morris, D. B. Holtkamp, S. J. Greene, and W. B. Cottingame, Phys. Rev. C24, 231 (1981).
57. E. Piasetzky, U. Sennhauser, H. W. Baer, J. D. Bowman, M. D. Cooper, H. S. Matis, H. J. Ziock, J. Alster, A. Erell, M. A. Moinester, and F. Irom (unpublished).
58. A summary of the data is given by P. A. Seidl et al., Phys. Rev. Lett. 50, 1106 (1983).
59. K. K. Seth et al., Phys. Rev. Lett. 43, 1574 (1979); and S. J. Greene et al., Phys. Lett. 88B, 62 (1979).
60. M. B. Johnson and H. A. Bethe, Commun. Nucl. Part. Phys. 8, 75 (1978); and J.-F. Germond and M. B. Johnson, Phys. Rev. C22, 1622 (1980).
61. M. B. Johnson and B. D. Keister, Nucl. Phys. A305, 461 (1978).

62. S. J. Greene, W. J. Braithwaite, D. B. Holtkamp, W. B. Cottingame, C. F. Moore, G. R. Burleson, G. S. Blanpied, A. J. Viescas, G. H. Daw, C. L. Morris, and H. A. Thiessen, Phys. Rev. C25, 927 (1982).
63. K. K. Seth, Proceedings of Intermediate Energy Nuclear Physics Workshop, June 21-27, 1980, Los Alamos National Laboratory report LA-8835-C.
64. L. C. Liu (unpublished).
65. V. A. Matveev and P. Sorba, Nuovo Cimento 45A, 257 (1978).
66. C. L. Morris, H. T. Fortune, L. C. Bland, R. Gilman, S. J. Greene, W. B. Cottingame, D. B. Holtkamp, G. R. Burleson, and C. F. Moore, Phys. Rev. C25, 3218 (1982); S. J. Greene, D. B. Holtkamp, W. B. Cottingame, C. F. Moore, G. R. Burleson, C. L. Morris, H. A. Thiessen, and H. T. Fortune, Phys. Rev. C25, 924 (1982); and R. A. Gilman et al., Phys. Rev. C (to be published).
67. S. J. Greene, W. J. Braithwaite, D. B. Holtkamp, W. B. Cottingame, C. F. Moore, G. R. Burleson, G. S. Blanpied, A. J. Viescar, G. H. Daw, C. L. Morris, and H. A. Thiessen, Phys. Rev. C25, 927 (1982).
68. M. B. Johnson, E. R. Siciliano, H. Toki, and A. Wirzba (unpublished).
69. D. Ashery et al., Phys. Rev. Lett. 47, 895 (1981).
70. B. D. Keister, Nucl. Phys. A271, 342 (1976); and M. K. Banerjee and S. J. Wallace, Phys. Rev. C21, 1996 (1980).
71. M. B. Johnson, Proc. Int. School of Physics, "Enrico Fermi," Course LXXIX, A. Molinari, Ed. (North Holland, Amsterdam, 1981), p. 412.